A MODIFICATION TO THE f-CHART AND $\bar{\phi}$,f-CHART METHOD FOR

SOLAR DOMESTIC HOT WATER SYSTEMS WITH STRATIFIED STORAGE

BY

ARTHUR BERNHARD COPSEY

A thesis submitted in partial fulfillment of the
requirements for the degree of

MASTER OF SCIENCE
(Engineering)

at the

UNIVERSITY OF WISCONSIN-MADISON

1984

ACKNOWLEDGEMENTS

I would like to thank my thesis advisors, Professors Bill Beckman and Sandy Klein for the suggestions and encouragement throughout this project. I am grateful for their help and the knowledge that they have both conveyed to me.

The friendship and camaraderie of the fellow RA's in the lab has made my stay here memorable and enjoyable. I wish you all the best of luck in your future harrassments. May all your DCM errors disappear.

Finally, the successful completion of this project would have been insurmountable without the selfless support of my wife, Donna. Her moral support and Love made the ups and downs more up and less down. Being married to a graduate student is a lonely event, and I thank you for your patience a million times over. Thanks, and more.

ABSTRACT

Several experimental and analytical studies have
recently indicated that SDHW performance can be enhanced by
operating the collectors at significantly lower flowrates
than currently practiced. These studies have shown that
system performance can be increased on the order of 10 to
15% by reducing the flow to about 20% of typical collector
flowrates. The f-Chart design method and the $\bar{\phi}$,f-Chart
design method are not applicable for SDHW systems operating
at low flowrates because they were developed with the
assumption that the tank is fully-mixed (a reasonable
assumption when conventional flowrates are used). A
modification to the f-Chart and $\bar{\phi}$,f-Chart methods were
developed by running numerous TRNSYS simulations employing a
stratified tank model. A correlation was developed between
collector flowrate and a dimensionless ratio, $\Delta X/\Delta X_{max}$.
From this ratio, a modified collector loss coefficient and
heat removal factor can be obtained. When these modified
parameters are used in a design method, the resulting solar
fraction is the performance that would be achieved from a
solar system with a stratified preheat tank. The methods
were compared with TRNSYS simulations in three locations:
Madison, Albuquerque, and Seattle. A range of collector

flowrates and load flowrates were also used. The RMS error of the annual solar fractions predicted by the design methods with the stratified tank modification relative to the the TRNSYS predictions was 2.07% for the $\overline{\phi}$,f-Chart method and 3.15% for the f-Chart method.

TABLE OF CONTENTS

LIST OF FIGURES

LIST OF TABLES

NOMENCLATURE

Symbols used in this thesis which do not appear below are
defined locally in the text.

A_s cross-section area of the storage tank

A_C collector area

C_p collector fluid specific heat

D tank diameter.

d_i inside riser tube diameter

d_o outside riser tube diameter

E collector effectiveness

F' collector efficiency factor

f_{max} monthly solar fraction for a solar system with a
           collector that has no thermal losses

f_{mix} monthly solar fraction for a solar system with a
           mixed preheat tank

f_{str} monthly solar fraction for a solar system with a
           stratified preheat tank

F_R collector heat removal factor

$\bar{H}_T$ monthly-average insolation incident upon the
           collector

H_o extraterrestrial radiation

H_s storage height.

I_c the critical radiation from equation 1.5

I_t	instantaneous radiation incident upon the collector per unit area
k	fluid thermal conductivity
K'_t	modified stratification coefficient, equation 1.12
K_s	stratification coefficient
$\overline{K}_T$	monthly-average daily clearness index
L	monthly energy removed from the system by the hot water demand
L_o	tank losses
$\overline{M}_c/M_L$	the ratio of daily collector flowrate to load flowrate
$\dot{M}_c$	collector mass flowrate
M_t	mass of fluid in the preheat tank
M	mixing number
N	number of days in the month.
N_p	collector operating time
P	tank perimeter
$Q_{a,c}$	auxiliary energy demand of a conventional DHW system
Q_a	auxiliary energy demand of the solar system
q_u	instantaneous rate of energy gain
Q_u	monthly-average daily useful energy gain
$\overline{R}$	monthly-average ratio of total radiation on a tilted surface to that on ahorizontal surface
R_n	noon radiation on the tilted surface to that on a

	horizonal surface for the average day of the month
r_{tn}	ratio of the total radiation in the hour around noon to the total daily radiation
T	storage tempertature
T_w	water set temperature
T_a	monthly-average ambient temperature
T_{day}	monthly-average temperature during the daylight hours
T_i	collector inlet water temperature
T_m	mains water temperature
T_o	the sunrise time if the sign is negative and the sunset time if it is positive.
T_{tank}	average storage temperature
T_∞	space temperature where the storage is located
U_t	storage loss coefficient
U_L	overall collector loss coefficient
U	inlet velocity
W	distance between riser tubes
X	X parameter for the f-Chart correlation, equation 3.1
X	vertical distance of the storage
X_c	monthly-average critical radiation level
Y	Y parameter for the f-Chart correlation, equation 3.2

ΔT	top-to-bottom temperature difference
Δt	number of seconds in the month
β_m	monthly optimal collector tilt, from Table 1.1.
β	collector tilt
β	fluid volumetric expansion
δ	the declination.
δ_p	absorber plate thickness
ϕ	the latitude
$\overline{(\tau\alpha)}$	monthly-average transmittance-absorption product
ω_s	sunset hour angle

CHAPTER ONE: INTRODUCTION

Recent studies have shown that the performance of solar
domestic hot water (SDHW) systems may be improved by
reducing the collector fluid flowrate. A high degree of
thermal stratification in the preheat tank may be achieved
in a system that has a low flowrate. Present design methods
assume that the storage tank is fully-mixed, a reasonable
assumption when high collector flowrates are used. A design
method that accounts for stratification is necessary to
evaluate SDHW systems operated at reduced flowrates. This
thesis investigated a modification to the f-Chart method and
the $\bar{\phi}$,f-Chart method to make them applicable to active SDHW
systems with thermal stratification. This chapter will
discuss the cause and effect of stratifed storage and
methods of obtaining the utilizability function, the
collector operating time, and the average ambient
temperature during daylight hours. The next chapters will
investigate modifications to present design methods to
account for stratification. Chapter Two presents a
correction based on the difference in solar fraction between
mixed tank and stratified tank systems. In Chapter Three, a
stratification modification for the f-Chart method is
presented. A correlation was developed between collector

flowrate and a modified collector loss coefficient. Finally, in Chapter Four the modified collector loss coefficient correction factor is applied to the $\bar{\phi}$,f-Chart method.

1.1 THERMALLY STRATIFIED STORAGE

Solar domestic hot water system are typically operated at relatively high collector flowrates. This control strategy results in a high value of the collector heat removal factor, F_R, and consequently a high collector efficiency. However, a high collector flowrate causes the fluid to be recirculated through the collector a number of times during a single day. Recirculation increases the average collector inlet temperature which reduces the collector efficiency. These are two opposite effects, high stratification at a low flowrate versus high F_R at a high flowrate, resulting in an optimal collector flowrate. This optimum has been demonstrated both both experimentally and analytically.

1.1.1 Effects of Reduced Collector Flowrate

The effect of collector flowrate on the monthly solar fraction for a fully-mixed preheat tank system is shown in Figure 1.1 . The decrease in performance associated with the decrease in flowrate is caused by the reduction of the heat removal factor.

A high collector flowrate does not necessarily mean that the solar domestic hot water system performance will be increased. High flowrates tend to reduce the degree of thermal stratification in the storage tank, since the fluid is recirculated through the collector a number of times per day and as a consequence, the average daily collector inlet temperature is increased. For a typical storage volume per collector area of 75 ℓ/m^2, the storage volume is recirculated through the collector three to five times per day. Recirculation causes fluid previously heated by solar energy to be pumped through the collector again, increasing collector losses. Simulations [1] and experiments [2] have shown that SDHW systems with typical storage volumes operated at high collector flowrates do not develop a high degree of stratification.
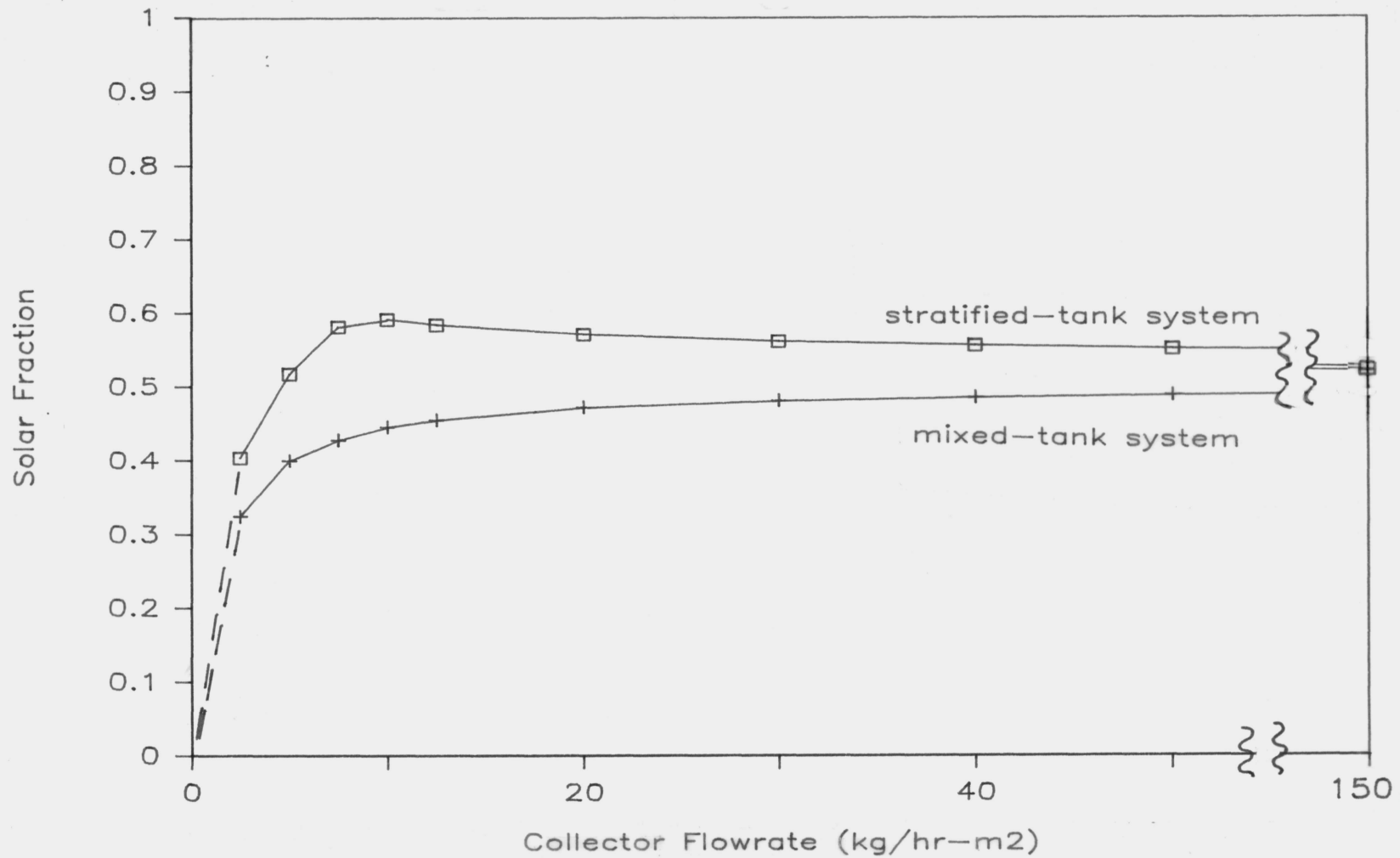
Figure 1.1   Effect of Collector Flowrate on the Theoretical, Monthly Solar Fraction
for a Stratified and a Fully-Mixed Preheat Tank System for the
Base Case System in Madison with a 300 ℓ/day Load.

4

The variation of solar fraction with flowrate per unit area for a stratified and a mixed tank system are shown in Figure 1.1 . At very low collector flowrates the performance of both systems is similar, due to the precipitous decline in F_R for very low flowrates. At high flowrates the performance of the stratified system approaches that of the mixed system. For stratified systems with a high collector flowrate, the large amount of recirculation causes the difference between the tank top and bottom temperatures to be small, so that the performance is close to that of the mixed tank system. The maximum difference in solar fraction between the two systems can be significant. From the results presented in this graph, the low-flow control strategy appears to perform better than the high-flow strategy. The rapid decrease in system performance at flowrates less than the optimal flowrate suggests that it may be advantageous to operate at a collector flowrate slightly greater than optimal.

1.2 DESIGN METHODS

Evaluating the long-term performance of a solar system is necessary to be able to choose the best system and to evaluate its economic merit. Detailed computer simulations,

such as TRNSYS [3], are one method by which the long-term system performance can be estimated. The advantages of detailed simulations are its flexibility and accuracy. The disadvantages are its high computer cost, necessary expertise, and required computer facilities. Except for unusual or very large systems, detailed computer programs are impractical as a long-term performance design tool. The results from these simulations, however, can be used in developing computationally simple design methods that use monthly-average meteorological data, rather than the hourly data required for TRNSYS. The long-term performance data obtained from these design methods are not as detailed or accurate as the data from simulations, but their accuracy is generally sufficient for design purposes. Two SDHW design methods were investigated in this study: the f-Chart method [4] and the $\bar{\phi}$,f-Chart method [5].

1.2.1 Conventional Solar Hot Water Heating Systems

Design methods are created for standard systems with a limited range of parameters. The parameter range is generally broad enough to incorporate the majority of system designs, but is limited to increase the accuracy for typical systems and to reduce the computational effort.

A typical open-loop solar domestic hot water system, for which the f-Chart method and the SDHW modification to the $\bar{\phi}$,f-Chart method are configured to, is shown in Figure 1.2. It is a two tank set-up with a pump circulating the fluid from the preheat tank through the collector. A relief value dumps fluid, and energy, if the average temperature of the preheat tank is above the fluid boiling point. A differential controller activates the pump if the temperature difference between the tank outlet and collector outlet is greater than a deadband temperature. A heat exchanger may be present between the collector and preheat tank, allowing an antifreeze solution to be circulated through the collector. The auxiliary tank boosts the water temperature to a desired set temperature, if necessary. Water is removed from the auxiliary tank to supply the load. During a hot water draw, mains water flows into the bottom of the preheat tank, and water from the top of the preheat tank flows into the auxiliary storage. If the delivery temperature is above the set temperature, a mixing valve mixes mains water with the delivery water to maintain the set temperature.

In open-loop designs, a load removes not only energy, but also fluid. This is in contrast to a closed-loop SDHW system, shown in Figure 1.3 . When a load is present, the
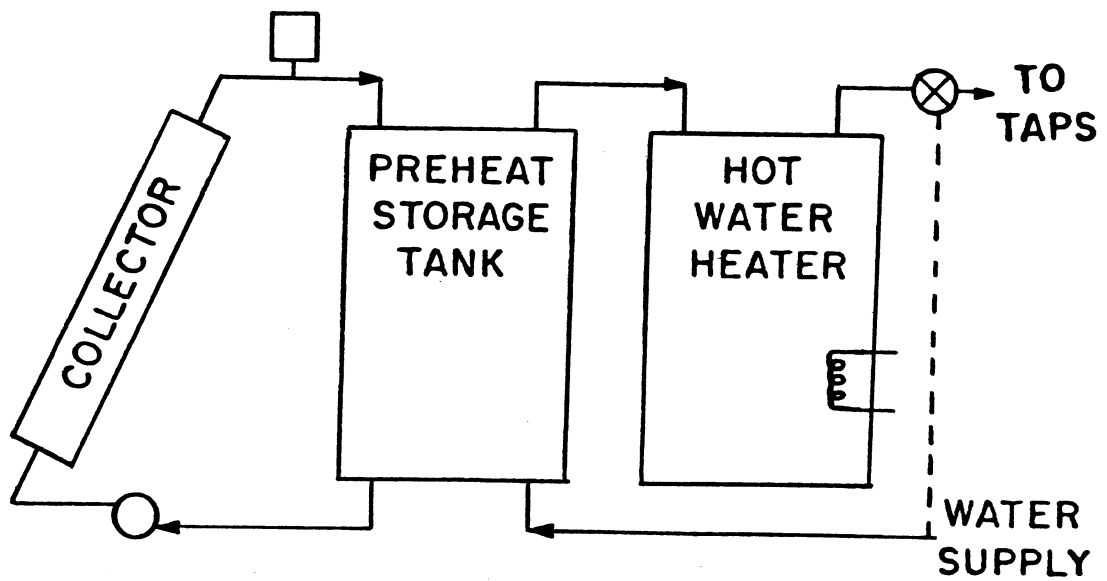
Figure 1.2   Open-loop Solar Domestic Hot Water System Schematic.
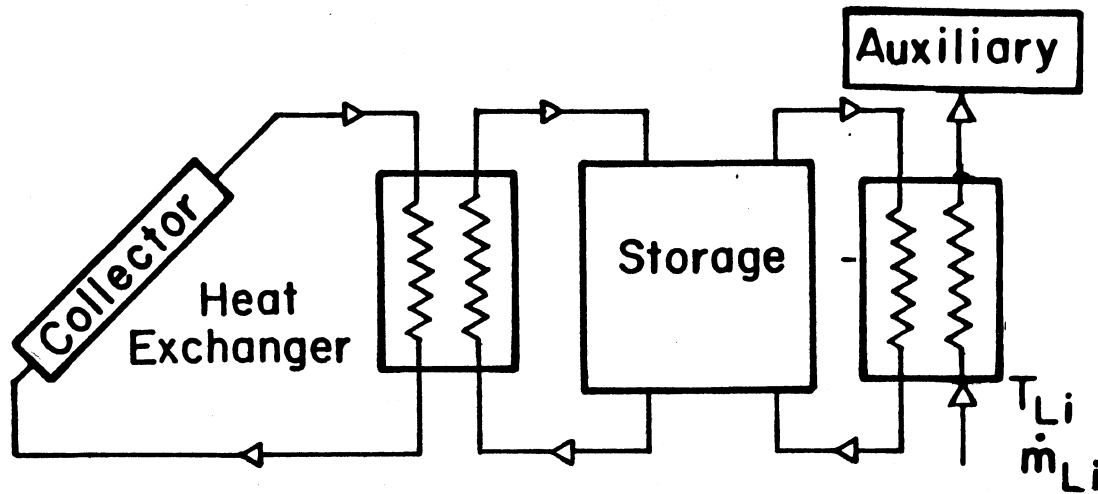
Figure 1.3   Closed-loop Solar Domestic Hot Water System
Schematic. From Reference [34].

heated liquid is pumped through a load heat exchanger. No mass is transfered between the solar system and the load. These systems are characterized by a single minimum temperature, T_{min}, above which useful energy is obtained. This system is the configuration upon which the $\overline{\phi}$,f-Chart design method [5] originally was based on.

1.2.2 Measures of System Performance

A measurement of system performance is necessary to quantitatively compare different systems. The rationale behind considering a SDHW system is economic, so a measure of performance could be the reduction in the amount of conventional fuel used. The fuel displacement is generally nondimensionalized by dividing by the load to give a "solar fraction." Depending upon the definition of the load, the solar fraction can have different values. Buckles and Klein [6] have investigated three solar fraction definitions

$$f_1 = 1 - \frac{Q_a}{L+L_o} \qquad [1.1]$$

$$f_2 = 1 - \frac{Q_a}{L} \qquad [1.2]$$

$$f_3 = 1 - \frac{Q_a}{Q_{a,c}} \qquad\qquad [1.3]$$

where,

Q_a auxiliary energy demand of the solar system

$Q_{a,c}$ auxiliary energy demand of a conventional

   DHW system

L hot water load

L_o tank losses

The first solar fraction definition, equation 1.1, defines the total load as the hot water demand plus the tank losses. This definition may not be appropriate for a measure of the fraction of displaced fuel, since the load of the solar system may be larger in a two-tank system due to preheat tank losses, than in a conventional system. Also, experimental tank losses are sometimes difficult to monitor due to conduction through the connecting pipes, thermal stratification in the storage, and temperature swings in the space where the storage is located.

The second solar fraction equation includes only the hot water load in the denominator. Tank losses are not ignored, since they will increase the auxiliary energy demand causing f_2 to decrease. If the solar energy collected is greater than the tank losses, f_2 can be

negative. Experimentally determining f_2 is easy since the auxiliary energy and the hot water load are easily measured.

From an economic standpoint, the system should be referenced to a conventional system that supplies the same quantity of hot water. The third solar fraction is the ratio of the supplied energy difference between a conventional and solar DHW system to the conventional system. Choosing a conventional system to compute $Q_{a,c}$ can be difficult, due to the differences between solar and conventional systems. For example, SDHW tanks are generally larger than conventional DHW tanks. In this study the solar fraction defined by equation 1.2 was used.

1.2.3 Utilizability

The instantaneous useful energy gain by a flat-plate collector is given by the well known Hottel-Whillier equation [7,8,9]

$$q_u = A_c F_R [(\tau\alpha)I_t - U_L(T_i-T_a)]^+ \qquad [1.4]$$

where,

q_u instantaneous rate of energy gain

A_c collector area

F_R collector heat removal factor

$(\tau\alpha)$ transmittance-absorbtance product

I_t instantaneous radiation incident upon the collector per unit area

U_L collector loss coefficient

T_i collector inlet temperature.

T_a ambient temperature

The plus superscript means that only positive values of the quantity within the sqare brackets are considered. This implies that a controller with a zero deadband operates the pump whenever useful energy can be obtained.

The solar radiation must be greater than a critical level before the absorbed energy exceeds the collector losses and useful output is produced. This critical radiation level, I_c, is found by setting q_u of the Hottel-Whillier equation equal to zero and solving for the solar radiation

$$I_c = U_L (T_i - T_a) / (\tau\alpha) \qquad [1.5]$$

The useful energy from equation 1.4 can then be rewritten as

$$q_u = A_c F_R (\tau\alpha) (I_t - I_c)^+ \qquad [1.6]$$

The monthly total useful energy gain, Q_u, can be obtained by integrating equation 1.6 over a month, assuming that the critical level and $(\tau\alpha)$ are constant

$$Q_u = A_c F_R (\overline{\tau\alpha}) \int^{\Delta t} (I_t - I_c)^+ dt \qquad \text{[1.7]}$$

If the integral is nondimensionalized by referencing it to the total radiation, then a defining equation is obtained for utilizability

$$\overline{\phi} = \frac{\int^{\Delta t} (I_t - I_c)^+ dt}{\int^{\Delta t} I_t dt} \qquad \text{[1.8]}$$

Utilizability is the fraction of the incident solar radiation that could be obtained as useful energy from a collector with an $F_R(\tau\alpha) = 1$, $F_R U_L = 0$, and a constant temperature difference between the collector inlet and ambient. The monthly-average daily useful energy gain from equation 1.7 can be rewritten as

$$Q_u = A_c F_R (\overline{\tau\alpha}) \overline{\phi} \overline{H}_t N \qquad \text{[1.9]}$$

where,

$\overline{H}_t$ monthly-average solar radiation incident upon the collector

$(\overline{\tau\alpha})$ monthly-average transmittance-absorbtance product

N   number of days in the month.

15

The value of $\bar{\phi}$ cannot be obtained solely from the total radiation level. Illustrated in Figure 1.4 are two sequences of three days with the same total radiation level. The utilizability is the ratio of the shaded area to the total area. The sequence, having identical radiation each day has a lower $\bar{\phi}$ value than the sequence of variable radiation. The effect of increasing the variation of incident radiation is to increase the monthly-average utilizability.

The distribution of the number of high and low radiation days has been shown by Liu and Jordan [10] to be a unique function of the monthly-average clearness index, $\bar{K}_t$, independent of month and location. Therefore, a utilizability correlation could account for the dependence of $\bar{\phi}$ on the radiation distribution by including $\bar{K}_t$. Using this information, Klein [11] found that $\bar{\phi}$ could be correlated to $\bar{K}_t$ and two dimensionless varibles, $\bar{R}/R_n$ and X_c.

$\bar{R}/R_n$ is a geometric factor that includes the collector tilt, location, and time of the year. $\bar{R}$ is the monthly ratio of radiation incident of a tilted surface to that on a horizontal surface. R_n is the noon ratio of radiation on the tilted surface to that on a horizontal surface for the average day of the month.
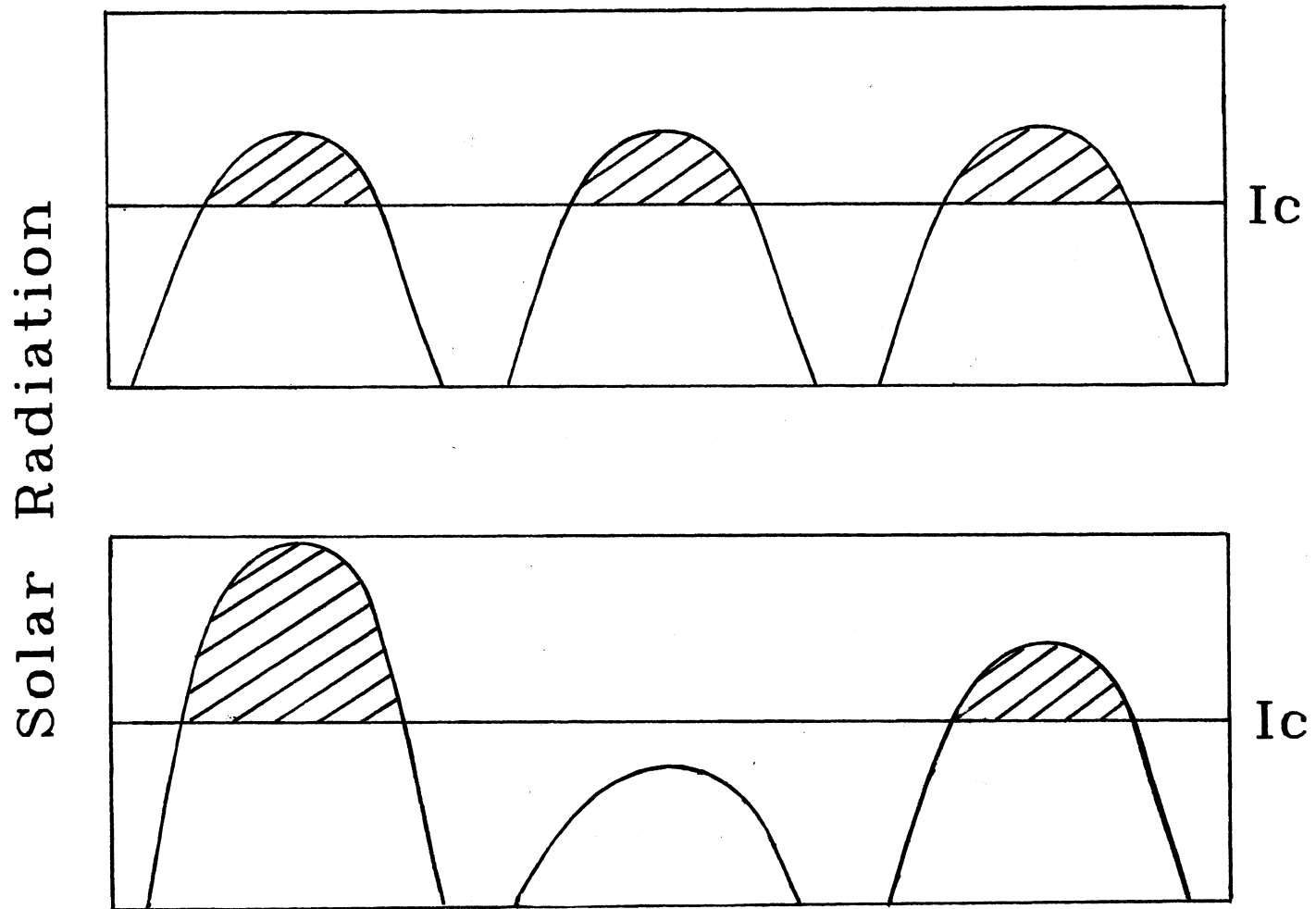
Figure 1.4   Two Sequence of Days with the same Average
Radiation.   From Reference [11].

The monthly-average critical radiation level, X_c, is the ratio of the critical level from equation 1.5 to the noon radiation level for the average day of the month

$$X_c = \frac{I_c}{r_{t,n} R_n \bar{K}_t H_o} \qquad [1.10]$$

Methods for obtaining the variables in the denominator can be found in Duffie and Beckman [12].

Klein's correlation for the monthly-average utilizability as a function of X_c, $\bar{R}/R_N$ and $\bar{K}_t$ is given by

$$\bar{\phi} = \exp[a+b(\bar{R}_n/R)][X_c+CX_c^2] \qquad [1.11]$$

where,

$$a = 2.943-9.271\bar{K}_t+4.031\bar{K}_t^2$$
$$b = -4.345+8.853\bar{K}_t-3.602\bar{K}_t^2$$
$$c = -.170-0.306\bar{K}_t+2.936\bar{K}_t^2.$$

The maximum error for this correlation is 2.5%.

Another relationship for $\bar{\phi}$ was developed by Evans, et al [13]. Equation 1.11 is accurate over a wide range of data, but requires the calculation of some computationally difficult terms. Evans' regression is computationally simpler than Klein's correlation and is given by

$$\bar{\phi} = 0.97 + AI_c + BI_c^2 \qquad [1.12]$$

where,

I_c the critical radiation from equation 1.5

$A = -4.86 \cdot 10^{-3} + 7.56 \cdot 10^{-3} K'_t$

$\quad - 3.81 \cdot 10^{-3} (K'_t)^2$

$B = 50.43 \cdot 10^{-6} - 1.23 \cdot 10^{-5} K'_t$

$\quad + 7.62 \cdot 10^{-6} (K'_t)^2$

$K'_t = \overline{K}_t \cos[0.8(\beta_m - \beta)]$

β collector tilt

β_m monthly optimal collector tilt, from Table 1.1.

This correlation has a reasonably low error for utilizability values greater than 0.6 (average RMS = 1.7%) but a larger uncertainty in smaller values of utilizability (average RMS = 2.8%). The value of the monthly-average collector inlet temperature used in calculating the critical level, equation 1.5, is often not known exactly. Therefore, the higher error of equation 1.12 may be offset by its calculation ease and the uncertainty of the input variables.

The utilizability design concept can be used whenever a collector operates at a known monthly critical level. If this is the case, then the useful energy gain can be obtained from equation 1.9. An example of a system that would be amenable to the utilizability design is a system with a very large storage so that the return temperature to the collector is nearly constant over a month. (seasonal storage). Generally, SDHW systems have a varying critical

Table 1.1 Values of the Tilt Angle to be used in
Equation 1.12, From Reference 12

Month	β_m
1	$\theta+29$
2	$\theta+18$
3	$\theta+3$
4	$\theta-10$
5	$\theta-22$
6	$\theta-25$
7	$\theta-24$
8	$\theta-10$
9	$\theta-2$
10	$\theta+10$
11	$\theta+23$
12	$\theta+30$

level and are not applicable to this method.

1.3 COLLECTOR OPERATING TIME

The number of hours that the collector pump operates is needed to calculate the parasitic energy requirement and the daily mass of fluid that is pumped through the collector. It will be shown in Chapter Three that the degree of thermal stratification present in a SDHW preheat tank is a function of the daily mass of fluid that is pumped through the collector. Obtaining the collector operating time analytically is not possible, even when the assumption of a perfect contoller is imposed. Some relationships for the collector operating time were investigated.

Mitchell, Theilacker and Klein [14] have developed a relationship for the pump-on time as a function of the monthly-average daily utilizability. A plot of a typical solar radiation level for a clear day is shown in Figure 1.5. A differential controller with a zero deadband will activate the pump whenever the radiation level reaches some critical level, I_c, at which time the collector losses are equal to the collector gains. The daily utilizability for this case is the area of the curve above the critical level divided by entire area. If the differential area bounded by
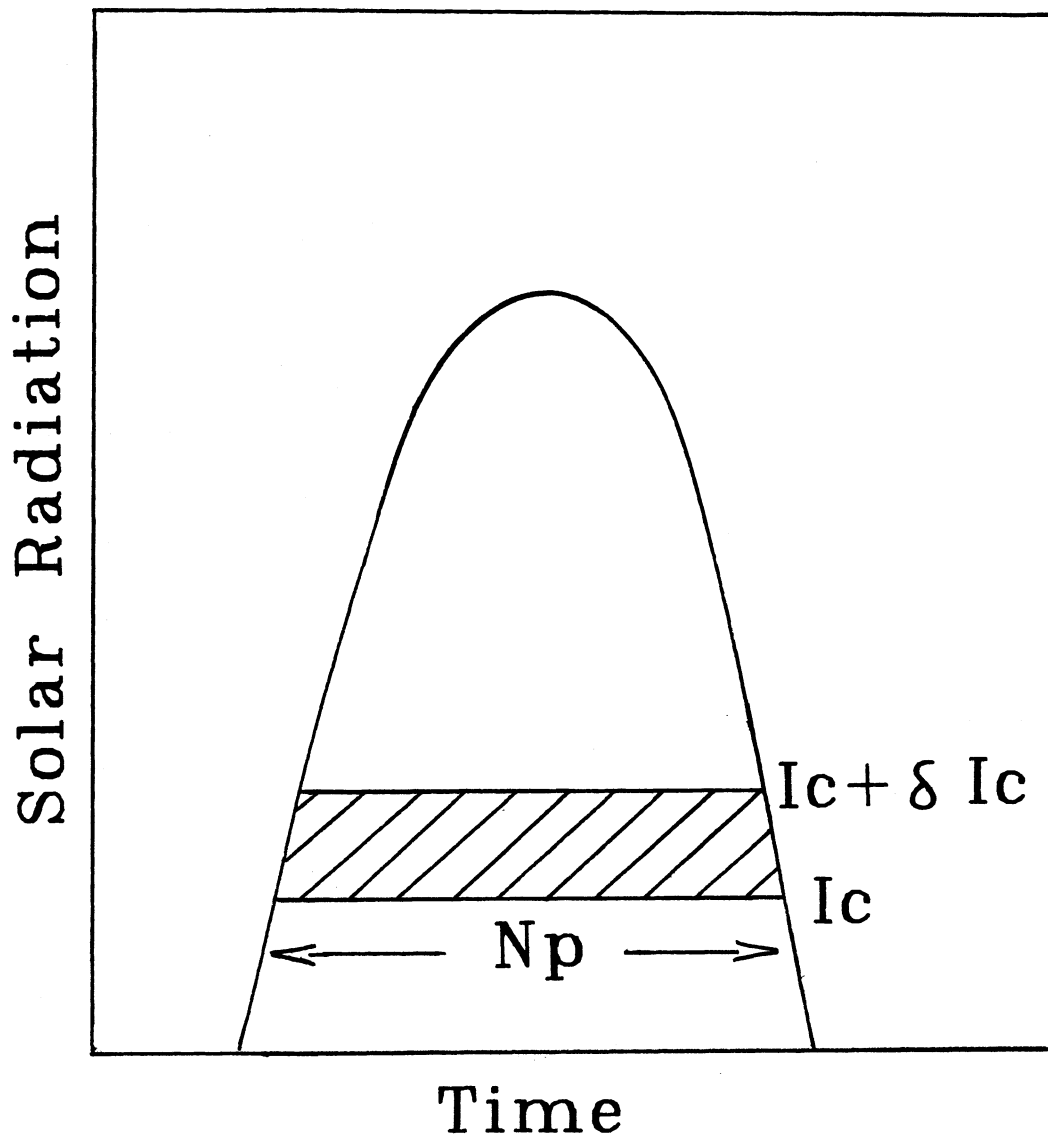
Figure 1.5   Radiation level for a Clear Day.   From
Reference [14].

I_c and the critical level plus a differential amount, $I_c+\delta I_c$, is approximated as a rectangle, then the monthly average daily pump operating time is

$$N_p = \bar{H}_t \frac{[\bar{\phi}(I_c)-\bar{\phi}(I_c+\delta I_c)]}{\delta I_c} \qquad [1.13]$$

In the limit as δI_c approaches zero, the right hand side becomes an exact differential

$$N_p = -\bar{H}_t \frac{d\phi}{dI_c} \qquad [1.14]$$

The difficulty in using equation 1.14 is in determining an appropriate critical level. To obtain a monthly-average daily collector operating time from equation 1.14, a monthly average collector inlet temperature, T_i must be used in equation 1.6, yielding a monthly-average critical level. The monthly-average collector inlet temperature cannot be obtained analytically. It is a function of the collector performance, mains water temperature, load distribution and quantity, and meteorological conditions. The collector inlet temperature is also a measure of the amount of tank recirculation. If the recirculation volume is small, then a reasonable approximation for the average inlet temperature would be the mains water temperature.

Evans' correlation was employed for determining the collector operating time for two reasons. First, using mains water temperature in the critical level evaluation will give relatively high utilizability values and this correlation has a low RMS error for high $\bar{\phi}$ values, and second, the computational effort involved in solving Evans' utilizability equation 1.12 is small. Taking the derivative of equation 1.12 results in an expression for the collector operating time, N_p, given by

$$N_p = \bar{H}_t (A + 2BI_c) \qquad\qquad [1.15]$$

where,

A and B are the same coefficients as given in
    equation 1.12.

There are a number of sources for error in the evaluation of the operating time. If the mains water temperature is lower than the ambient temperature, the collector inlet temperature is low, and the contoller deadband is small, then the pump may operate at night. The useful energy gain during this nighttime operation is small, but the operating time can be large enough to cause an error in the pump-on time estimation. This behavior is often observed for thermally stratified storage systems that have a low collector inlet temperature. Another error source is

the assumption that the collector inlet temperature is equal to the mains water temperature. This may be a good assumption for stratified tank SDHW systems, but not for fully-mixed storage designs. A third error is numerical. The intergration of a numerically derived correlation tends to decrease the error, while differentiation tends to increase the uncertainty. This will cause the RMS error for the collector operating time to be greater than the utilizability correlation error.

A plot of the monthly-average collector flowrate for a mixed storage tank obtained from TRNSYS compared to the results from equation 1.15 are shown in Figure 1.6 . The bias is caused by the collector inlet temperature always being greater than or equal to the mains water temperature. For the mixed tank system in Madison simulated in Figure 1.6, the collector did not operate at night, since the collector inlet for a mixed tank is generally higher than the ambient temperature at night. A similar plot is shown in Figure 1.7, comparing stratified storage simulations with the results from equation 1.15 . The bias observed in the previous graph is not as evident in this plot, since the stratified storage tank causes the perfect controller (zero turn-on and turn-off deadbands) to operate when the sun is not up, due to the low collector inlet temperature of the
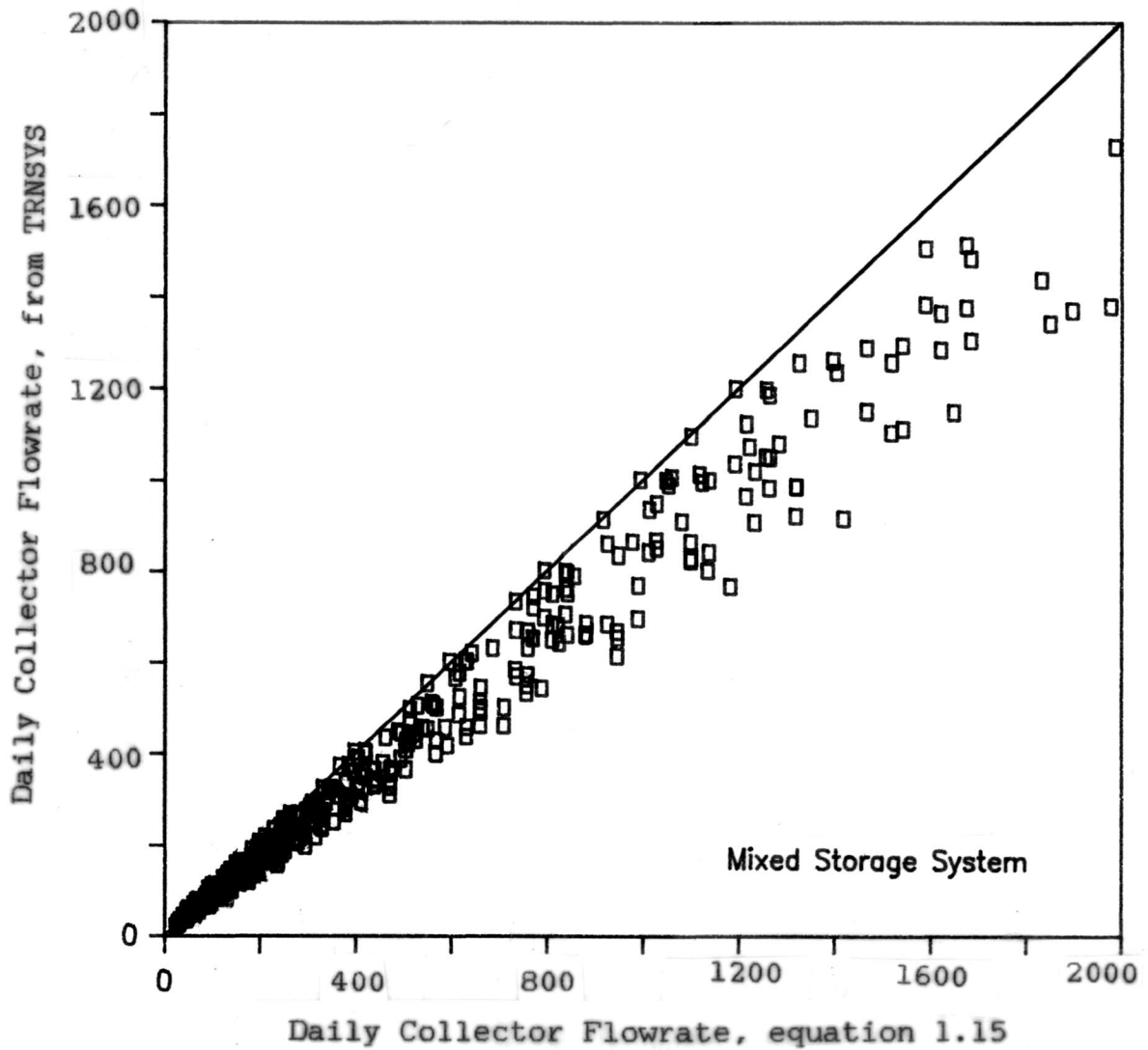
Figure 1.6   Monthly-Average Daily Collector Flowrate from
Simulations with a Mixed Preheat Tank Compared
to Equation 1.15.
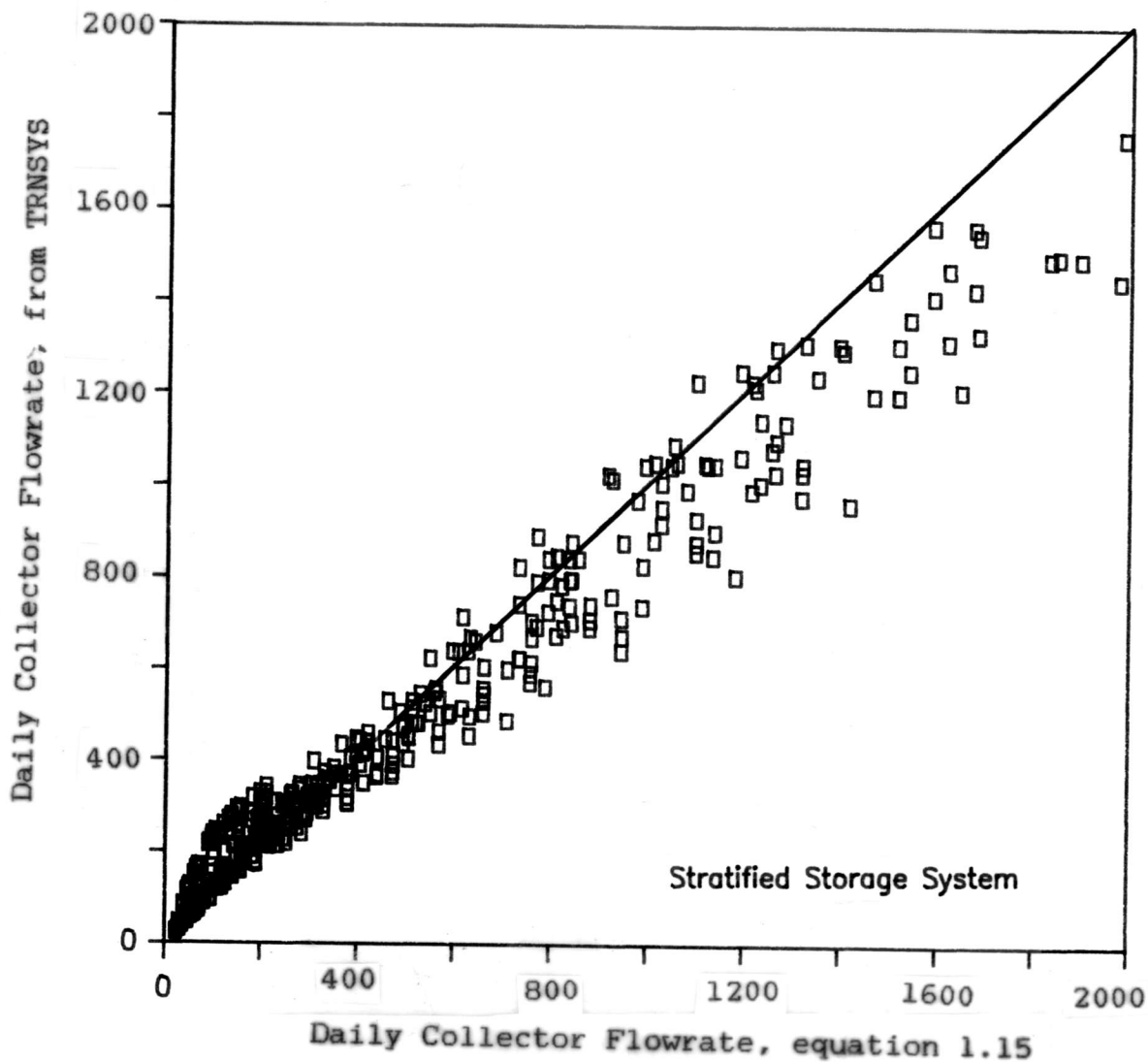
Figure 1.7   Monthly-Average Daily Collector Flowrate from
Simulations with a Stratified Preheat Tank
Compared to Equation 1.15.

stratified tank.

The collector operating time can also be evaluated by using a correlation for the monthly-average daily utilizability developed by Klein [11]. As mentioned before, this equation is more computionally involved than Evans' correlation, but more accurate over a wide range of critical radiation levels. Evaluating the derivative of Klein's ϕ equation to obtain the collector operating time produces

$$N_p = -\bar{\phi}[A + B(\bar{R}_n/R)][1. + 2CX_c] \bar{R}/(r_{tn} R_n) \qquad [1.16]$$

where,

$\bar{\phi}$, A, B, and C are from equation 1.11, and

R_n, r_{tn}, and $\bar{R}$ can be obtained

from Duffie and Beckman [12].

A program that inplements the $\bar{\phi}$,f-Chart method, such as F-CHART4.1 [15], requires the evaluation of the variables needed for equation 1.16 . For these programs, evaluation of equation 1.16 is not difficult, since most of the input variables are previously calculated.

Other collector operating time relationships were also investigated. An attempt was made to find an equation that did not require utilizability, so that the computational effort could be reduced. The pump-on time variation with the number of daylight hours can be approximated as being linear for a limited set of data. For a wider range of

data, the relationship appeared to be a function of solar fraction. A correlation was developed relating the collector operating time to the daylength and solar fraction. This correlation was found to work well for equations that are not sensitive to the accuracy of the pump operating time. Since they are a function of the daylength, they are location biased. For this reason, collector operating time correlations depending upon the daylength were not used in this study.

1.4 AVERAGE DAYLIGHT AMBIENT TEMPERATURE

The monthly-average critical level is obtained from equation 1.5 using monthly-average collector inlet temperature and ambient temperature. The ambient temperature that should be used in the monthly-average critical level equation is the temperature that the collector is exposed to during the day while it is operating. The ambient temperature that is usually available in meteoroliqical data is not the daytime temperature, but rather the mean value for the day and night.

Erbs [16] has developed a relationship for the monthly-average hourly temperature, $T_{a,h}$, as a function of the monthly-average clearness index, $\overline{K}_t$, and the monthly-average ambient (day and night) temperature, T_a,

$$T_{a,h} = T_a + A[0.4632\cos(t*-3.805)$$
$$+ 0.0984\cos(2t*-0.360) + 0.0168\cos(3t*-0.822)$$
$$+ 0.0138\cos(4t* - 3.513)] \qquad [1.17]$$

where

t = time in hours, with 1 corresponding to 1 am

$t* = \pi(t-1)/12$

$A = 25.8\overline{K}_t - 5.21$

This relationship can be integrated from sunrise to sunset to give a value for the monthly-average daylight temperature. The sunrise or sunset time is obtained from the sunset hour angle, ω_s, in radians as

$$T_o = \pm 12\omega_s/\pi \qquad [1.18]$$

where,

T_o the sunrise time if the sign is negative and the sunset time if it is positive.

The sunset hour angle can be found from Reference [12]

$$\omega_s = \arccos(-\tan\phi \tan\delta) \qquad [1.19]$$

where,

ϕ the latitude

δ the declination.

Integrating equation 1.17 over a day with the limits obtained from equation 1.18 yields the monthly-average daylight temperature, T_{day},

$$T_{day} = T_a + (A/\omega_s) \cdot$$
$$[2.129\sin(\omega_s) + 0.238\sin(2\omega_s)$$
$$+ 0.002\sin(3\omega_s) - 0.004\sin(4\omega_s)] \qquad [1.20]$$

This formula does not give the actual value for the average ambient temperature during operation unless the collector operates from sun-up to sun-down. The average ambient (day and night) temperature is lower than the average operation temperature, and equation 1.20 will lie between these extremes. If the solar radiation level is high, then the average daylight temperature will be closer to the average operation temperature, while if the temperature amplitude, A, from equation 1.17 is large and the solar radiation level is low, the difference between the operating temperature and daylight temperature could be large. The average daylight temperature is closer to the operating temperature than the average day and night temperature, so it is a better approximation for T_a in the monthly-average critical level evaluatione.

1.5 OBJECTIVES

The objective of this research was to develop a general design method for domestic hot water heating systems that have a thermally stratified tank. The approach that was taken was to find a relationship between a fully-mixed tank parameter and the corresponding stratified tank parameter.

Chapter two analyzes previous work that has been done attempting to analytically develop a measure of stratification. Also in Chapter Two, an empirical solar fraction modification is analyzed.

In Chapter Three, modifications to the f-Chart method are discussed. A correction factor was developed that modifies variables in the X and Y parameters, so that the solar fraction obtained from the f-Chart method is the performance that would be achieved from a stratified-tank system. The stratification correction that was found to have the lowest error over the widest range of parameters modified the collector loss coefficient and the heat removal factor. The performance of a SDHW system with a stratified preheat tank can be obtained by using the modifed U_L and F_R in the f-Chart method.

The collector loss coefficient modification is applied to the $\overline{\phi}$,f-Chart method in Chapter Four. Therefore, stratified tank domestic hot water systems can be analyzed with this design method.

CHAPTER TWO: SOLAR FRACTION MODIFICATION

There are many different approaches that could be undertaken to create a design tool for solar domestic hot water (SDHW) systems with stratified storage. A direct approach would be to start from basic principles and create a new design method. The advantage to this approach would be that the range of parameters relevant to stratified tank SDHW systems could be employed in determining the correlation, increasing the design method's applicability and possibly resulting in high accuracy. The disadvantage would be getting solar designers to learn to use a new design tool. There are a number of accurate, adaptable, and well known mixed-tank SDHW design methods presently available. Instead of adding another method for estimating solar fraction, the approach taken was to establish a correction for the existing tools. This correction could take a number of forms. One way would be to modify the implicit variables of the design method. This approach is utilized in some design methods, such as the $\overline{\phi}$,f-Chart method to account for open-loop systems and the f-Chart method to modify for different heat exchanger effectivenesses. Another technique for correcting existing design tools would be to find a relationship between the

solar fractions for mixed and stratified systems. The benefit of such a correction factor is its applicability for all SDHW design methods. The difficulty in a technique such as this lies in the nonlinear relation of solar fraction to other system variables. A correction factor involving solar fraction directly has been investigated analytically and empirically.

2.1 ANALYTICAL METHODS

A number of researchers have attempted to derive an analytical model to predict the effect of stratified storage on solar system performance. An analytical model could have the advantage of a relatively short computational time and if the simplifying assumptions were justifiable, good agreement with experimental results. The approach taken to develop an analytical model entails finding a solution to the partial differential equation for the one-dimensional heat transfer in a liquid storage tank with no load flow. The boundary conditions are an energy balance at the tank inlet and no temperature gradient at the tank bottom, and the initial condition is a given initial temperature distribution.

2.1.1 Stratification Coefficient

Phillips, et al. has studied stratified storage for air systems [17], and obtained integrated daily performance predictions of both air systems [18], and liquid-based solar systems [19]. He uses a dimensionless variable, the stratification coefficient, K_s, in solving the heat transfer equation. The stratification coefficient is defined as the ratio of the useful energy gain from a thermally stratified storage to the energy gain from an otherwise identical mixed-tank system. Employing the Hottel-Whillier equation, the stratification coefficient can be written as

$$K_s = \frac{A_c F_R [(\tau\alpha) I_t - U_L (T_i - T_a)]}{A_c F_R [(\tau\alpha) I_t - U_L (T_{tank} - T_a)]}$$ [2.1]

where,

T_i temperature of the bottom of a stratified tank

T_{tank} average tank temperature

If the stratification coefficient were known, then the instantaneous energy gain of a stratified tank solar system could be obtained by knowing the mean storage temperature, T_{tank}.

Phillips and Dave [19] were able to solve for a daily

K_s with the following assumptions: no tank losses, constant storage cross section, no hot water draw, one dimensional heat-transfer, and thermal inversion avoidance by placing the fluid entering the tank at the location with a temperature closest to its own. Separation of variables was used to obtain ordinary differential equations from the heat transfer equation. In order to solve the ordinary differential equation, it was assumed that the number of tank turnovers is large. The validity of this assumption is not immediately obvious. Phillips and Dave compare their results with detailed daily simulation, and for fairly high flow-rate systems, the analytical model agrees well with simulations. For systems with less than two tank turnovers per day and a collector effectiveness (equation 2.3) of greater than 0.2, the stratification coefficient can have a significant error, as shown below. It appears that systems with a low-flow control strategy will be outside of the acceptable collector effectivness and tank turnover range.

The general solution for K_s is iterative utilizing two dimensionless variables. The mixing number, M, is defined as

$$M = \frac{A_s\ k}{m\ C_p\ H_s} \qquad\qquad [2.2]$$

where,

A_s storage cross sectional area

k   fluid conductance

m   storage mass flowrate

H_s storage height.

For a 300 ℓ, 1.5 m tall storage tank with a low-flow control strategy collector flowrate of 10 kg/hr·m^2, the mixing number is 0.0016. The second dimensionless variable is the collector effectiveness defined as

$$E = \frac{F_R U_L A_c}{m C_p} \qquad\qquad [2.3]$$

For a collector with an $F_R U_L$ of 5 W/m^2 °C, and a flowrate of 10 kg/hr·m^2, the collector effectiveness is 0.43 .

The general solution to the stratification coefficient is the root of the equation

$$4pq(1-E)e^p = (p+q)^2 e^p - (p-q)^2 e^{-q} \qquad\qquad [2.4]$$

where,

$p = 1./(2M)$

$q = \sqrt{1.-EMK_s}\ /(2M)$

If the mixing number is small, then the stratification coefficient may be approximated as

$$K_s = \frac{\ln [1/(1-E)]}{E\{1+M \cdot \ln [1/(1-E)]\}}.$$ [2.5]

This agrees with the general solution to within one percent if the mixing number is less than 0.1. For vertical tanks, the mixing number will generally be much less than 0.1, so equation 2.5 should give reasonable results for the stratification coefficient.

The stratification coefficient versus collector flowrate, as calculated from equation 2.5, is shown in Figure 2.1 . Also on this graph are the ratios of monthly solar fractions from TRNSYS for a stratified and mixed system. Although the stratification coefficient was derived for instantaneous useful energy gains, Phillips and Dave compared it to daily simulation results. However, it is monthly average-daily results which are needed for SDHW design methods. The difference between the analytical results and simulated results shown in Figure 2.1 is significant. The large error at flows less than 20 kg/hr·m^2 is due primarily to the initial assumption of a large collector flowrate. Phillips and Dave state that most well designed systems have an $\overline{M}_c/M_L$ ratio much larger than one, which is contrary to findings by Veltkamp [20], von Koppen [21], Wuestling [22], and others.
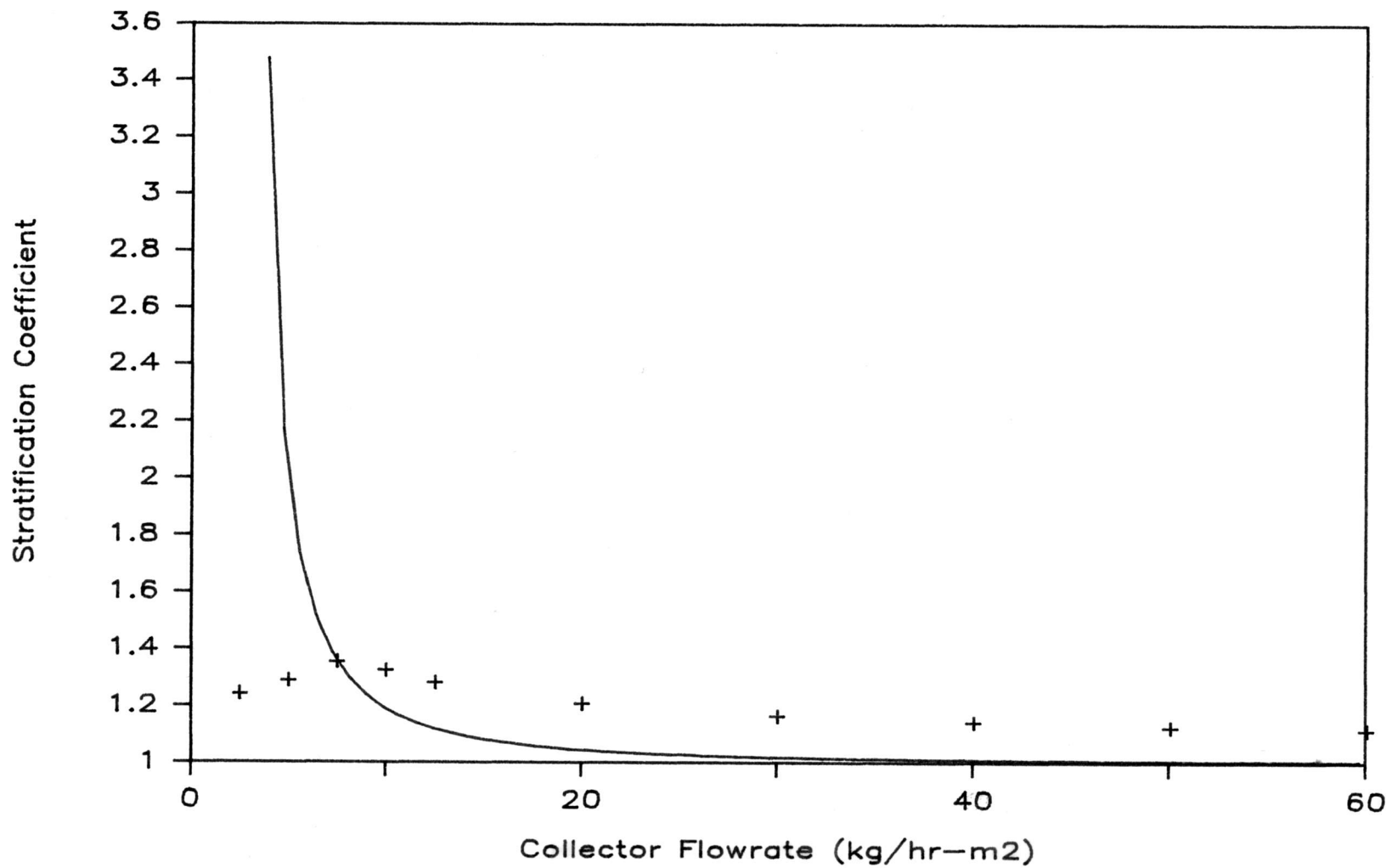
Figure 2.1   The Stratified Coefficient Compared with the
              Ratio of Stratified Tank Solar Fraction to
              Mixed Tank Solar Fraction from TRNSYS.

In summary, the stratification coefficient appears to work well for systems with fairly large collector to load flow ratios and no load, but the restrictions necessary with their analysis do not lend it well to a general design method.

2.1.2 Stratification Index

Cole and Bellinger [1] have analytically evaluated thermal stratification of liquid solar systems. They have developed a computationally involved storage model that includes a correlation for entrance mixing and conduction down the tank walls. They defined a stratification index that ranges from zero for a fully mixed tank to one for a perfectly stratified (no recirculation) tank. The stratification index from their equation compares well with experimental results. They experimentally and analytically investigated the effect of tank height, diffusers, dip tubes, baffles, and thermal wall capacity on tank stratification. They analyzed a parameter that measures the ability of a system to become and remain stratified. This dimensionless parameter is called the Richardson number

$$Ri = g\beta L\Delta T/U^2$$

$$= Gr\ Re^{-2}(H_s/D)^{-2} \qquad\qquad [2.6]$$

where,

g   gravitational constant

β   fluid volumetric expansion

H_s tank height

ΔT   top-to-bottom temperature difference

U   inlet velocity

D   tank diameter.

A large Richardson number indicates that the storage tank will remain stratified. The factors that cause a system to have a stratified storage are a large height to diameter ratio, a large temperature difference between the top and the bottom of the tank, and a low inlet velocity. Turner [23] indicates that convective mixing will occur for systems that have a Richardson number less than the critical value of 0.25. The inlet and outlet mixing is governed by the value of the Richardson number. It is interesting to note that Lavan and Thompson [24], who were apparently unaware of the significance of the Richardson number, empirically derived a correlation for measuring stratification that included

$$Gr\ Re^{-1.6}\ (H_s/D)^{-1.7} \qquad\qquad [2.7]$$

which is similar to equation 2.6 .

Although Cole and Bellinger's work would be valuable to a tank designer interested in increasing stratification, it is not useful in a design tool for predicting solar fraction, since it yields instantaneous rather than monthly quantities, it cannot deal with hot water draws, and it cannot deal with tank losses.

2.2 EMPIRICAL METHODS

An attempt was made to empirically derive a relationship between the mixed tank and stratified tank solar fractions. The approach taken was to correlate the stratified-tank solar fraction to a function involving the mixed-tank solar fraction.

2.2.1 Effect of Collector Flowrate on the
Heat Removal Factor

The values of $F_R U_L$ and $F_R(\tau\alpha)_n$ are affected by collector flowrate through the relationship of F_R with collector flowrate per unit area. The analytic relationship between F_R and collector flowrate is shown in Figure 2.2 and may be expressed as
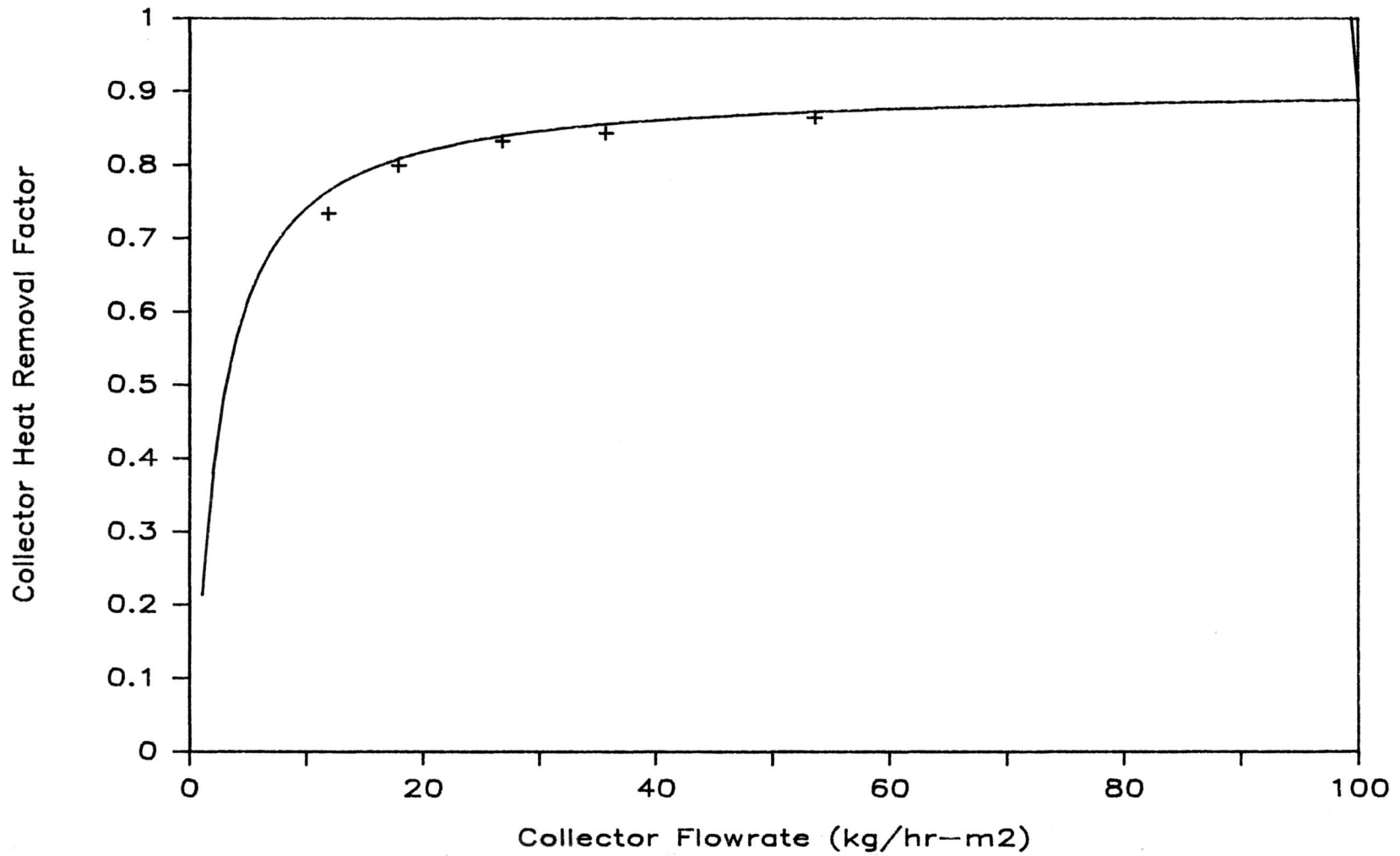
Figure 2.2   Comparison of Experimental and Analytical
Results Showing the Variation of F_R with
Collector Flowrate.

$$F_R = \frac{\dot{M}_c C_p}{A_c U_L} \left[1 - e^{-(A_c F' U_L / \dot{M}_c C_p)} \right] \qquad [2.8]$$

where,

    F'   collector efficiency factor

The collector efficiency factor, F', is a weak function of flowrate since the collector flowrate affects the convective heat transfer coefficient. The fluid flow in the riser tubes of liquid collectors is generally laminar. A flowrate of 0.04 kg/s through twenty 1 cm riser tubes yields a Reynolds number of approximately 500, well into the laminar region. For fully-developed internal laminar flow, the Nusselt number is independent of flowrate and the entrance effects are generally insignificant, due to the large length to diameter ratio of typical riser tubes. For the range of collector flowrates studied (2.5-60 kg/hr$\cdot$m^2), the collector efficiency factor changes by only one percent.

If F' is assumed independent of collector flowrate, then F_R can be modified for any liquid flowrate using an analytical correction ratio derived in reference [12]. For a given heat removal factor at test conditions, F_R at use conditions can be determined from

$$\frac{F_{R\ use}}{F_{R\ test}} = \frac{\dfrac{\dot{M}_c C_p}{A_c U_L}\left[1-e^{-(A_c F'U_L/\dot{M}_c C_p)}\right]\Bigg|_{use}}{\dfrac{\dot{M}_c C_p}{A_c U_L}\left[1-e^{-(A_c F'U_L/\dot{M}_c C_p)}\right]\Bigg|_{test}} \qquad [2.9]$$

where $F'U_L$ can be evaluated at the test conditions

$$F'U_L = \frac{\dot{M}_c C_p}{A_c}\,\ell n\left[1-\frac{A_c F_R U_L}{\dot{M}_c C_p}\right] \qquad [2.10]$$

Fanney [25] has experimentally investigated the degradation of collector performance caused by reduced flowrates. A comparison of his experimental results and equation 2.9 is shown in Figure 2.2 . The difference between the experimental and analytical procedures is small, due possibly to the uncertainty of the low flow measurement.

2.2.2 Identification of Important Parameters

The first step in developing a correlation is to find the relevant parameters. The omission of parameters that the function is dependent upon may not increase the error for a limited set of data; however, it will cause the correlation to be biased at the extreme parameter values. An example of this is the f-Chart assumption that the storage is fully-mixed and the solar fraction strictly

increases with collector flowrate (assuming no pipe losses.)
For high collector flowrates this assumption is valid, but
as the flowrate is reduced and the tank becomes stratified,
the design method underpredicts the system performance.

Stratification in vertical tanks is not strongly
dependent upon the storage tank height to diameter ratio.
Vertical tanks generally have a Richardson number that is
much larger than the critical value, so inlet mixing is not
significant. Also, the conduction between fluid segments is
generally not significant for vertical tanks [26].

Wuestling [22] found that the stratified-tank solar
fraction depends upon the collector flowrate, load flow, and
the storage volume. As discussed in Section 1.1, stratified
systems perform better than mixed systems due to the reduced
collector inlet temperature. The stratified system
performance degrades when the warm fluid returning from the
collector is recirculated through the collector, increasing
losses. To maximize the performance, the collector flowrate
should be as high as possible to increase F_R, but low enough
to avoid recirculation. This is achieved by pumping through
the collector on a daily basis a volume of fluid
approximately equal to the volume removed by the hot water
draw. If the daily flowrate is higher than the daily load,
recirculation will occur; and if it is lower, the collector
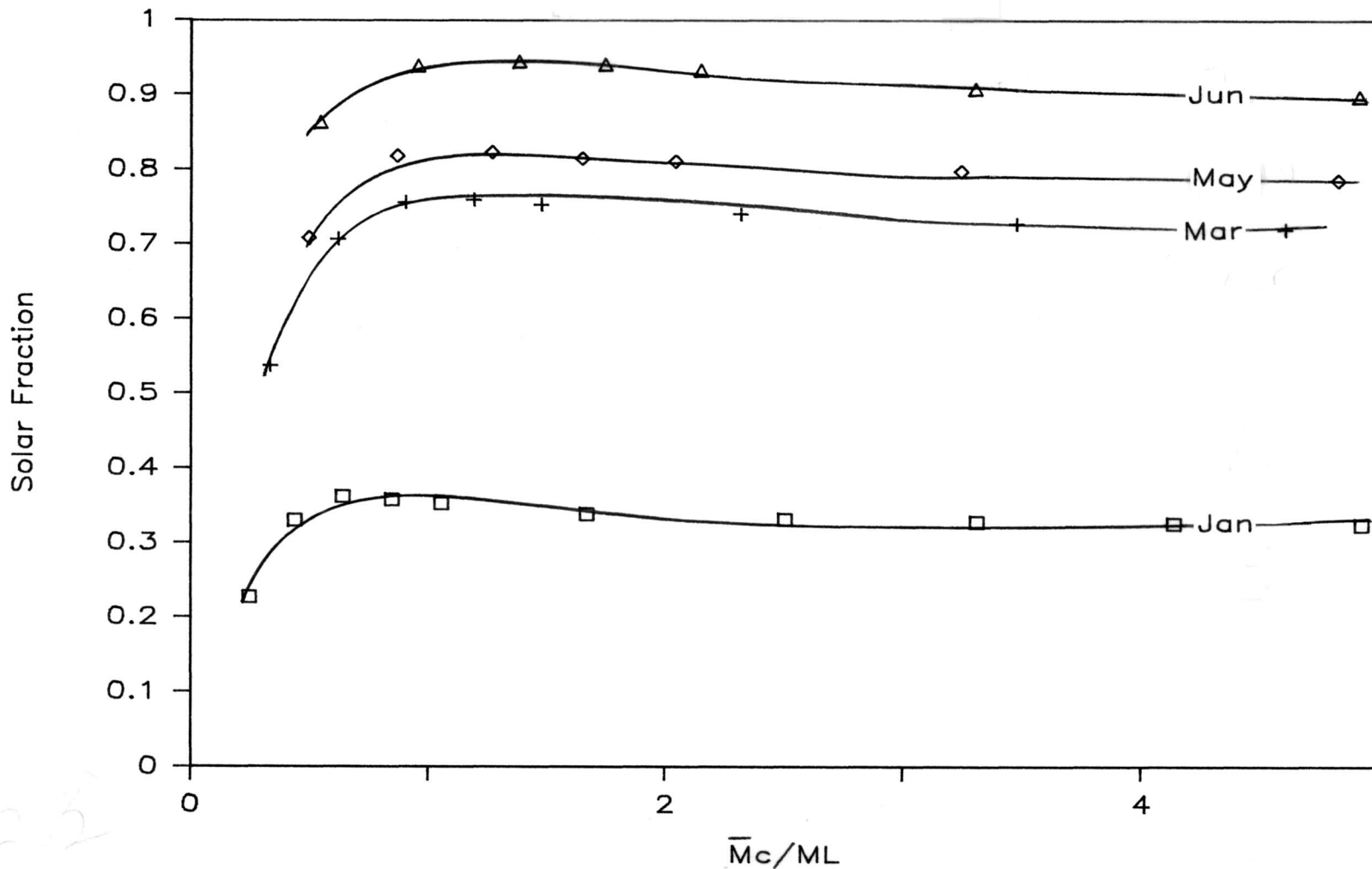
Figure 2.3   Solar Fraction Variation with the Ratio of
              Monthly-Average Daily Collector Flow to Daily
              Load Flow.

efficiency is poor due to a low heat removal factor.

To achieve maximum performance, the volume of the storage tank should be large enough to avoid recirculation, but small enough to reduce tank losses. Wuestling has shown that well-insulated tanks with a volume as least as large as the daily collector flowrate will achieve a similar performance.

The variation of solar fraction from a stratified-tank system with the collector flowrate per unit area was shown in Figure 1.1. For the reasons discussed above, the optimal collector flowrate will depend upon the load, as indicated in Figure 2.3. This graph shows that the optimal system performance occurs when the monthly-average daily collector flowrate, $\overline{M}_c$, is approximately equal to the monthly-average daily load flow, M_L. Wuestling examined the effect of other variables on the optimal solar fraction. The parameters that were investigated include location, collector quality, tank loss coefficient, controller deadband, collector area, set temperature, daily load, and load distribution. Although the solar fraction varied considerably, the daily collector flowrate that yielded the maximum solar fraction appeared to be fairly independent of the parameters.

2.2.3 System Description

A range of parameters were investigated to ensure the design method's validity for typical solar systems. The load flows examined range from 200 ℓ/day to 400 ℓ/day, covering most domestic daily draws. The load profile used was the RAND [27] profile, which is a representative draw pattern. Domestic load profiles vary considerably. Even for a particular residence, variation can be observed from day to day depending upon the operation of high hot-water demand appliances. The effect of load distributions for fully-mixed storage tanks has been examined analytically by Buckles and Klein [6] and experimentally by Fischer and Fanney [28]. They conclude that load profiles have a small effect on the thermal performance of SDHW systems with typical storage tank volumes operated at high flowrates. They found that the optimal system performance was achieved with designs that removed energy from the tank during collector operation. This control strategy tends to reduce the collector inlet temperature for mixed tanks, decreasing collector and storage losses.

Wuestling [29] analyzed the effect of draw patterns on stratified tank systems, investigating eight different profiles. He found that the RAND profile achieved an average solar fraction when compared to the other draw

patterns. The best performance was achieved by an afternoon
draw. Removing the useful energy in the afternoon reduces
recirculation and preheat tank losses since the average tank
temperature is generally highest in the afternoon. The
worst performance was registered by a late morning draw that
caused the most recirculation and tank losses. The maximum
difference in solar fraction between the best or the worst
draw pattern and the RAND profile was 5%. Including the
load pattern in a design method would be difficult since the
draw profile is a difficult parameter to quantify. The RAND
profile is a typical draw pattern and was observed to have a
performance for stratified tanks between the other profiles.
It was, as a result, employed in this study.

The weather data used were SOLMET typical
meteorological year (TMY) data [30]. Madison, WI, Alb-
uquerque, NM, and Seattle, WA were the locations that were
explored. These three places cover a wide range of
clearness indices and ambient temperatures. The regions
studied are not a group of three typical cities, but rather
a range of the meteorological extremes. There are few
places except Albuquerque in June that have a $\overline{K}_t$ of 74%, and
few cities with the exception of Seattle in December that
have a $\overline{K}_t$ of 29%. Madison has wide annual weather swings,
with clearness indices ranging from 0.38 to 0.55 and ambient

temperature changing from -7°C to 21°C. Most other regions' weather statistics should fall between these extremes, providing a test for for location independence in this design method.

Three flat-plate collector designs were analyzed. The base-case system was a three collector array, each module being single glazed with low iron glass and having a selective surface absorber plate. The high loss system was polymer single glazed without a selective surface, and the low loss system was a double glazed selective surface design. The collector efficiency factors for the three systems, along with the other system parameters, are listed in Table 2.1. These three systems cover a wide range of collector types. Referencing the SRCC directory [31] showed that only 1% of certified liquid flat-plate collectors are outside of the range listed in Table 2.1.

A wide range of instantaneous collector flowrates were employed in this analysis. As shown by Wuestling [22], a change in collector flowrate of only 3 $kg/hr \cdot m^2$ near the maximum solar fraction can result in a 12% change in monthly solar fraction. For this reason, a range of flowrates near the maximum solar fraction was used to increase the method's accuracy. High collector flowrates were used so that the solar fraction from a stratified tank

Table 2.1 Parameter Values for the Systems Simulated in this Study

Locations — Madison, WI; Albuquerque, NM; Seattle, WA

Collectors
$A_c = 4.2 \text{ m}^2$

$\dot{M}_c(\text{test}) = 71.5 \text{ kg/hr m}^2$

slope=latitude

$b_o = 0.1$

Base Case
$F_R U_L = 4.73 \text{ W/m}^2\text{C}$

$F_R(\tau\alpha)_n = 0.805$

Higher Quality
$F_R U_L = 3.62 \text{ W/m}^2\text{C}$

$F_R(\tau\alpha)_n = 0.754$

Lower Quality
$F_R U_L = 8.57 \text{ W/m}^2\text{C}$

$F_R(\tau\alpha)_n = 0.697$

$M_c = 2.5, 5, 7.5, 10, 12.5,$
$20, 30, 40, 50, 60 \text{ kg/hr m}^2$

Preheat Tank
Volume=0.30 m^3

Height=1.5 m

$U = 0.42 \text{ W/m}^2\text{C}$

Auxiliary Tank — negligible losses

Hot Water Load
Demand=200, 300, 400 ℓ/day

$T_m = 10 \text{ C}$

$T_w = 60 \text{ C}$

$T_\infty = 20 \text{ C}$

system will approach the solar fraction from a mixed storage system at high collector to load flow ratios. Ten flowrates ranging from 2.5 to 60 kg/hr·m^2 were used as inputs to TRNSYS. The collector flowrate that yielded the optimal system performance generally was between 10 and 20 kg/hr·m^2.

2.2.4 Component Model Description

The transient systems simulation program, TRNSYS 12.1 [3] was employed to simulate SDHW systems. The elements of the solar systems were modeled with standard TRNSYS components.

The algebraic, plug-flow tank model was used for the preheat tank [32]. The plug-flow model uses a number of variable sized constant temperature segments of fluid to simulate stratification. The algebraic tank model does not have to solve a set of simultaneous equations, therefore it is more computationally efficient than a finite difference, multi-node model. A description of the model is shown in Figure 2.4, in which a series of temperature profiles are plotted. The top profile is the initial temperature distribution at time t_1. If collector flow occurs during a timestep, then a plug of fluid is inserted in the top of the

54
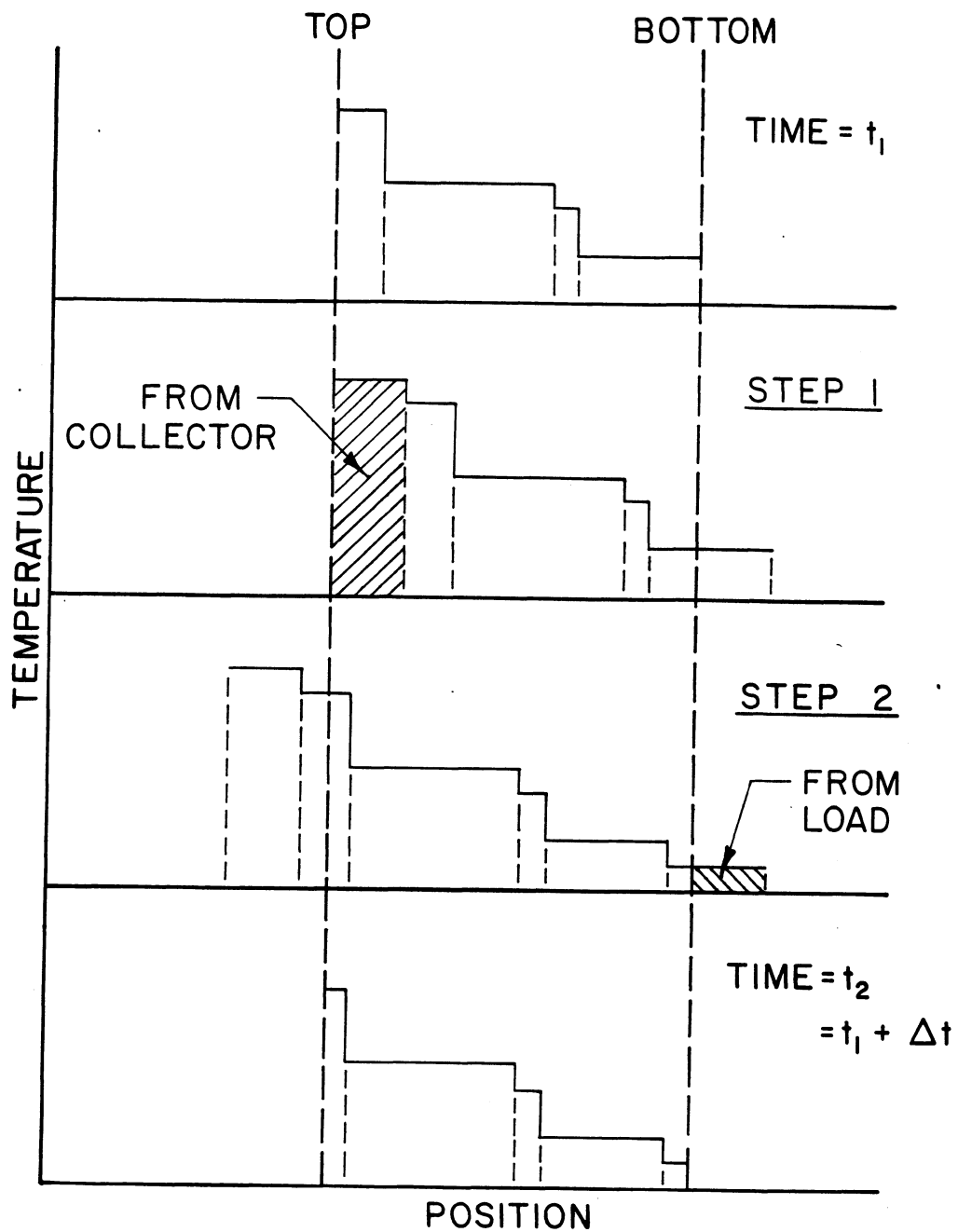
Figure 2.4 Operation of the Plug-Flow Storage Tank Model. From Reference [29].

tank, and fluid from the tank bottom is returned to the collector, shown in step 1. A load flow removes fluid from the top of the tank and returns mains water into the bottom, shifting the segments towards the top of the storage. Tank losses are calculated individually for each segment. Internal mixing between segments is not considered. This model has two modes of operation. The variable inlet position mode inserts the fluid returning from the heat source or the load between segments of adjacent temperatures to avoid temperature inversions. This mode yields an upper limit on tank stratification, the lower limit being a fully-mixed storage. The fixed inlet position mode combines adjacent segments when the collector fluid return temperature is lower than the fluid temperature at the top of the tank. The fixed inlet position was chosen for the simulations used here since it appears to agree better with a limited set of low-flow experimental data [26].

The pump was activated by a perfect controller (i.e. having zero turn-on and turn-off deadbands). The auxiliary tank contained a 9 kW auxiliary heater and was assumed to be fully mixed. The water mains temperature and set temperature were constant at 10°C and 60°C respectively. A relief valve allowed boiling to take place, and a tempering valve maintained the set temperature by mixing the

hot water with mains water as necessary.

2.2.5 Δf Correlation

The difference between the mixed and stratified tank solar fractions versus the collector to load ratio is shown in Figure 2.5. The maximum value for these curves is not at a collector to load flow ratio of one like the stratified tank solar fraction, but at a value slightly less than one. The maximum for the Δf function will occur where

$$\frac{d\Delta f_{str}}{d(\bar{M}_c/M_L)} = 0 \qquad\qquad [2.11]$$

For the strictly increasing mixed tank solar fraction function, the maximum difference between the mixed tank and stratified tank systems will generally occur at a collector to load flow ratio less than the collector to load flow ratio that maximizes the stratified tank solar fraction. The exception is if the mixed tank solar fraction reaches one, then the maximum will occur at the lowest collector to load flow ratio for which the stratified tank solar fraction is one.

The curves in Figure 2.5 are approximately the same shape with the maxima occuring at about the same collector to load flow ratio. If these curves are normalized by
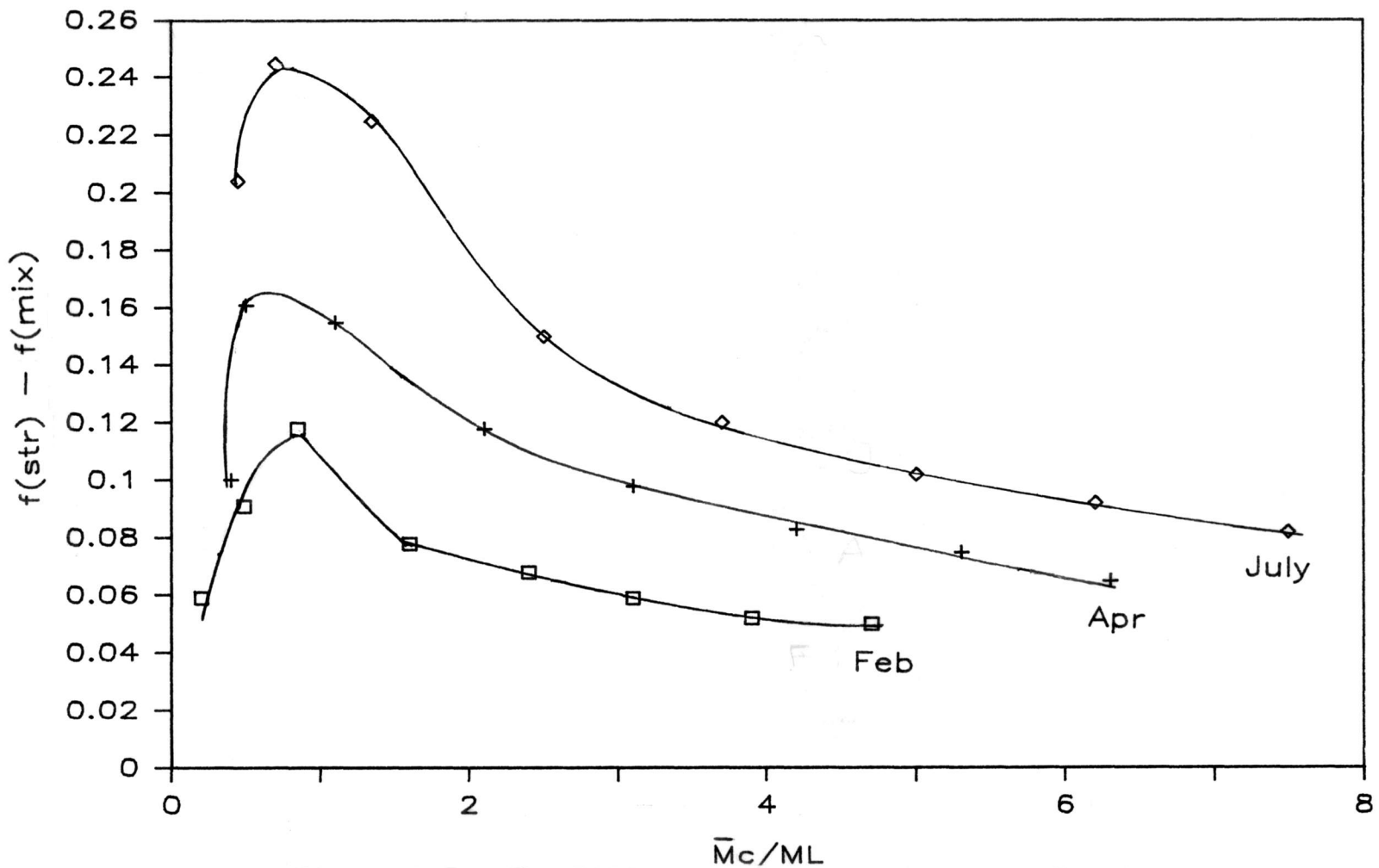
Figure 2.5   The Difference Between the Mixed-Tank and Stratified-Tank Solar Fraction Variation with the Ratio of Monthly-Average Daily Collector Flow to Daily Load Flow for the Base Case System in Madison with a 300 ℓ/day Load.

dividing by their maximum solar fraction difference, Δf_{max} value, a single curve is generated, as shown in Figure 2.6. The strategy for developing a design method for low flowrates is to find an equation for the maximum difference between the stratified **and mixed tank solar** fraction, and develop a correlation **for** $\Delta f / \Delta f_{max}$, **as shown** in Figure 2.6. The stratified tank solar **fraction could be** obtained from this method once a mixed tank solar fraction was obtained from a design method such as the f-Chart method.

The maximum solar fraction difference will be a function of the average tank temperature. If the monthly-average tank temperature is equal to the mains water, then Δf_{max} is zero since the auxiliary energy will be equal to the load for the stratified tank and mixed tank systems. If the monthly-average tank temperature is equal to the desired set temperature, the maximum solar fraction difference is also zero since the auxiliary energy demand is also zero for both the stratified and mixed storage systems. Between these extremes, the maximum difference is a finite, positive quantity due the improved performance of the stratified tank design over the mixed tank system. The mixed-system solar fraction is a linear function of the monthly-average tank temperature. A plot of the maximum difference between the
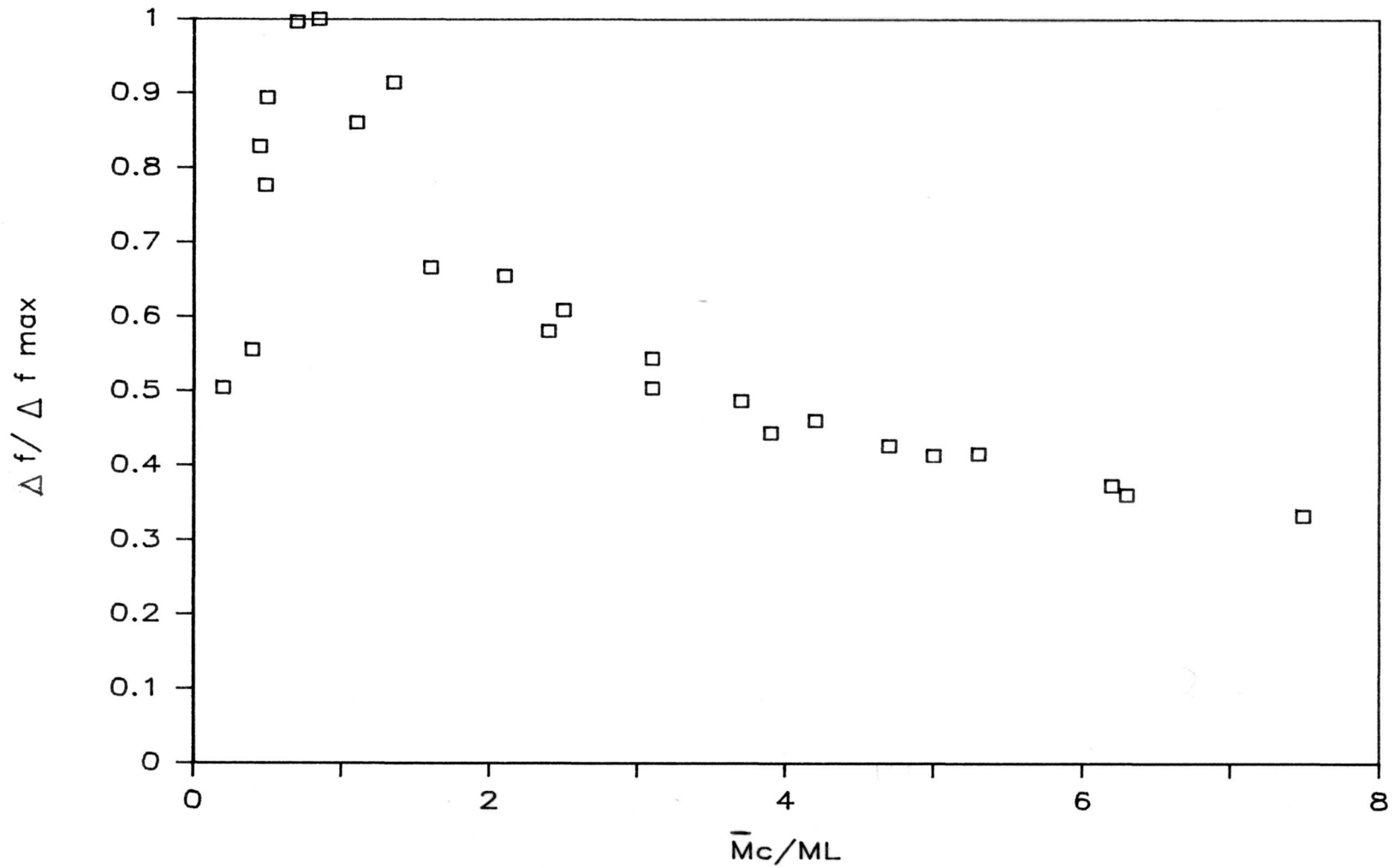
Figure 2.6 $\Delta f/\Delta f_{max}$ Versus $\overline{M}_c/M_L$ for the Base Case System in Madison with a 300 ℓ/day Load.

mixed-system and stratified-system solar fraction versus the mixed-tank solar fraction at the flowrate that yields Δf_{max} is shown in Figure 2.7. The relationship is fairly linear at low solar fractions, but due to energy dumping, Δf approaces zero as the mixed tank solar fraction approaces one. A similar plot is shown in Figure 2.8. This time the independent variable is the stratified-system solar fraction at the flowrate that yields Δf_{max}. This curve has less scatter, and the trend is linear. The wide range of Δf_{max} data for a stratified-system solar fraction of one is due to energy dumping. A linear regression for Figure 2.8 with the stratified-system solar fraction constrained to be less than 0.99

$$\Delta f_{max} = 0.322 \ f_{str} \qquad \qquad [2.12]$$

with a correlation coefficient of 87%. The stratified system solar fraction was used to correlate the maximum solar fraction difference instead of the mixed-system solar fraction due to the linear relationship between f_{str} and Δf_{max}.

A function was chosen that exhibits the same behavior as the $\Delta f / \Delta f_{max}$ relationship shown in Figure 2.6. This function is zero for a collector flowrate of zero, has a maximum at $\overline{M}_c / M_L$ of slightly less than one, and
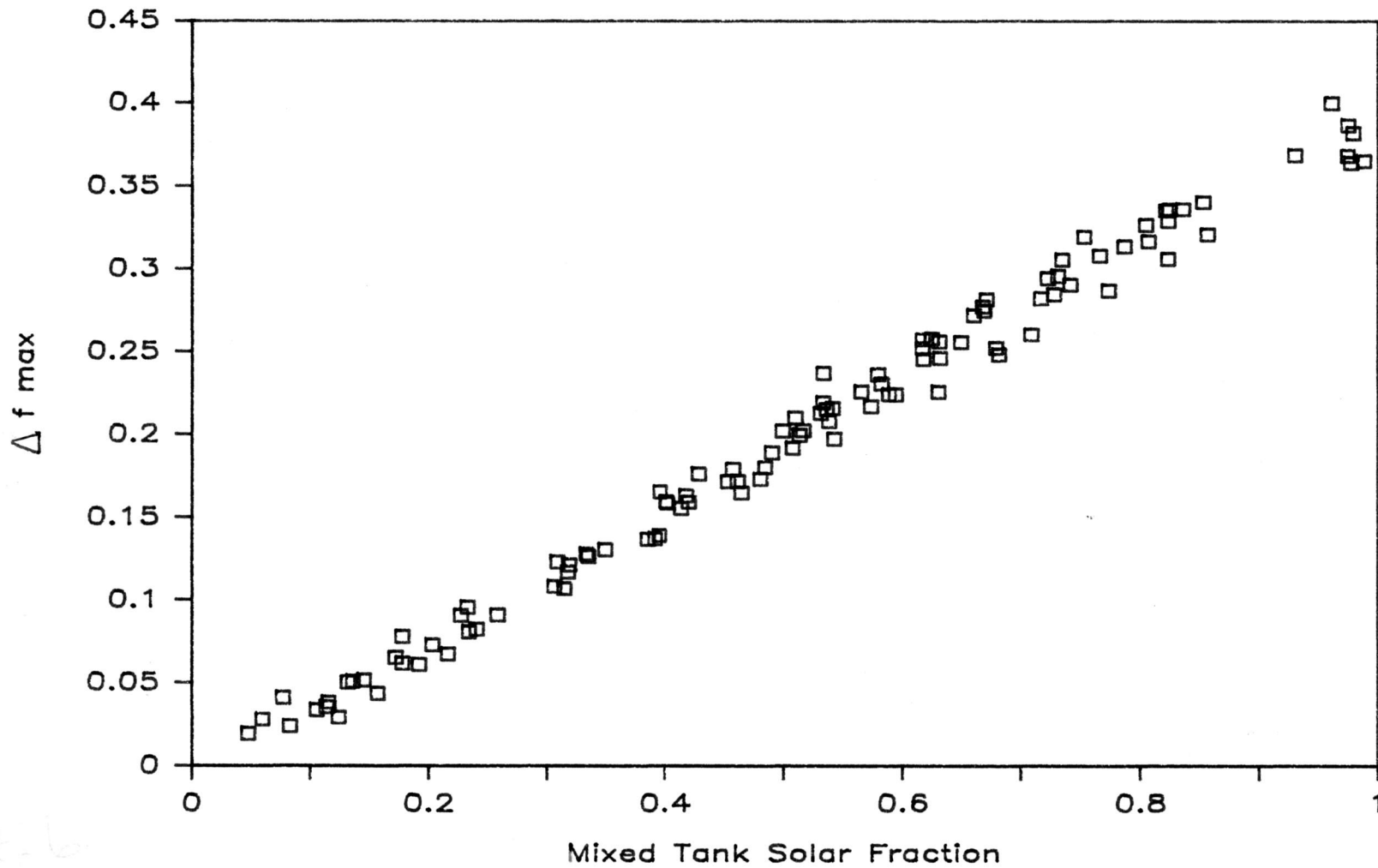
Figure 2.7 Δf_{max} Variation with the Mixed-Tank Solar Fraction for the Base Case System in Albuquerque.
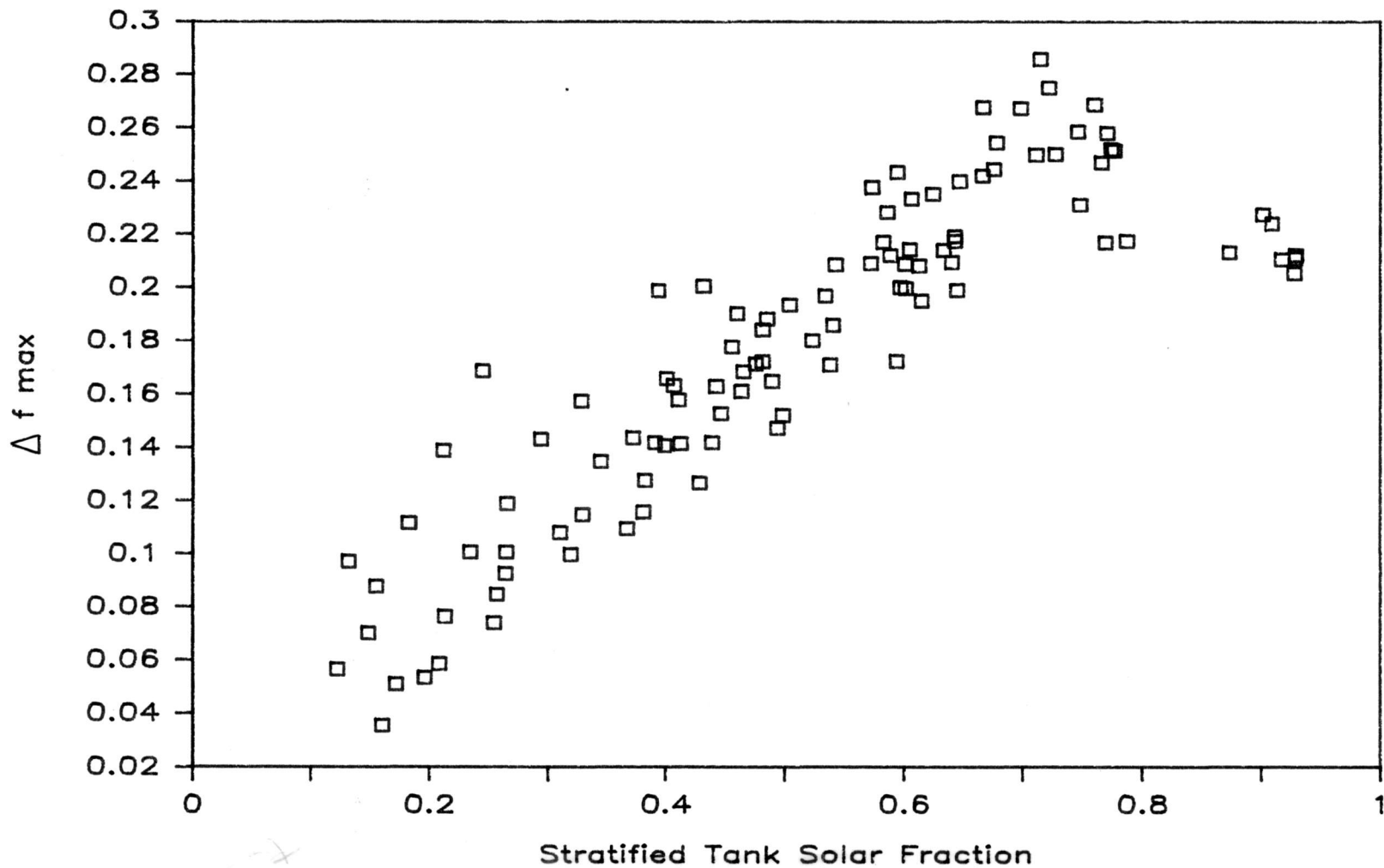
Figure 2.8 Δf_{max} Variation with the Stratified-Tank Solar Fraction for the Base Case System in Albuquerque.

asymptotically approaches zero as the collector to load flow increases. A function that exhibits this behavior is

$$\frac{\Delta f}{\Delta f_{max}} = C_1 M \exp(C_2 M + C_3 M^2) \qquad [2.13]$$

A nonlinear regression routine was then used to find the relationship between $\Delta f / \Delta f_{max}$ and collector to load flow ratio.

The stratification correction is noniterative, even though the stratified-system solar fraction is used to correlate Δf_{max}. To use the method, the derivative of equation 2.13 is used to find the collector to load flow ratio that yields Δf_{max}. This collector flowrate is used in the f-Chart method to give the mixed-tank solar fraction at Δf_{max}. Then Δf_{max} is obtained from equation 2.12 using the mixed-tank solar fraction, since the only unknown is the stratified-system solar fraction. Equation 2.13 is then used at the actual flowrate to give the stratified-system solar fraction.

The RMS error between TRNSYS simulations and the Δf correlation for Madison with 10 collector flowrate and 3 load flows is 6.9% for monthly solar fractions and 4.7% for annual values with a bias of 2.7%. There are a number of reasons for the large error. The maximum solar fraction difference varies with the collector loss coefficient. A

stratified tank system has a better performance than a mixed-tank design due to the lower collector inlet temperature. Therefore, decreasing the collector loss coefficient will reduce the solar fraction difference between a mixed and stratified system.

Also, the relationship between $\Delta f / \Delta f_{max}$ and the collector to load flowrate is a function of the time of the year. During the winter, the high instantaneous collector flowrate that yields the maximum difference between the stratified and mixed systems is relatively high. This causes recirculation to be obtained at a lower $\overline{M}_c/M_L$ and tank losses to be increased.

Due to the high error of the Δf correlation, another approach was taken. A solar fraction difference is difficult to correlate due to its nonlinear behavior and the large number of variables that it is dependent upon. In the next chapter, a stratified tank modification is studied which modifies one or more variables that are used in the f-Chart method.

CHAPTER THREE: MODIFICATION TO THE F-CHART METHOD

FOR THERMALLY STRATIFIED SDHW SYSTEMS

In this chapter, a modification to the f-Chart method to account for stratified storage is presented. First, a correction factor based on an equivalent collector area is explored. The equivalent collector area is the collector area that a fully mixed system would need to obtain the same solar fraction as an otherwise identical stratified tank system. The collector area modification agrees well with simulations for the system that it was designed for, but it has a high error for SDHW systems with different collector parameters. A more general stratification correction factor is then presented. This modification is based on the collector loss coefficient, and it agrees well over the wide range of parameters that were tested.

3.1 REVIEW OF THE F-CHART METHOD

The f-Chart method is the most well known, widely used design method for residential solar heating systems [4]. The solar fraction is calculated from correlations which were developed from hundreds of TRNSYS simulations. Correlations were developed for liquid space heating, air

space heating, and domestic hot water systems. The system for which the SDHW correlation was based on is shown in Figure 1.2.

The solar fraction for SDHW systems was correlated to two dimensionless variables. The X parameter is related to the ratio of the collector losses to the load and is given by

$$X = \frac{A_c F_R U_L (11.6 + 1.18 T_w + 3.86 T_m - 2.32 T_a) \Delta t}{L} \qquad [3.1]$$

where,

T_w water set temperature

T_m mains water temperature

Δt number of seconds in the month

The dimensionless Y parameter is related to the ratio of absorbed radiation to the load and is given by the relation

$$Y = \frac{A_c F_R (\overline{\tau\alpha}) \overline{H}_t N}{L} \qquad [3.2]$$

The relation between solar fraction for SDHW systems and the X and Y parameters is shown in Figure 3.1 or from the least squares approximation

$$f = 1.029Y - 0.065X - 0.245Y^2 + 0.0018X^2 + 0.0215Y^3 \qquad [3.3]$$
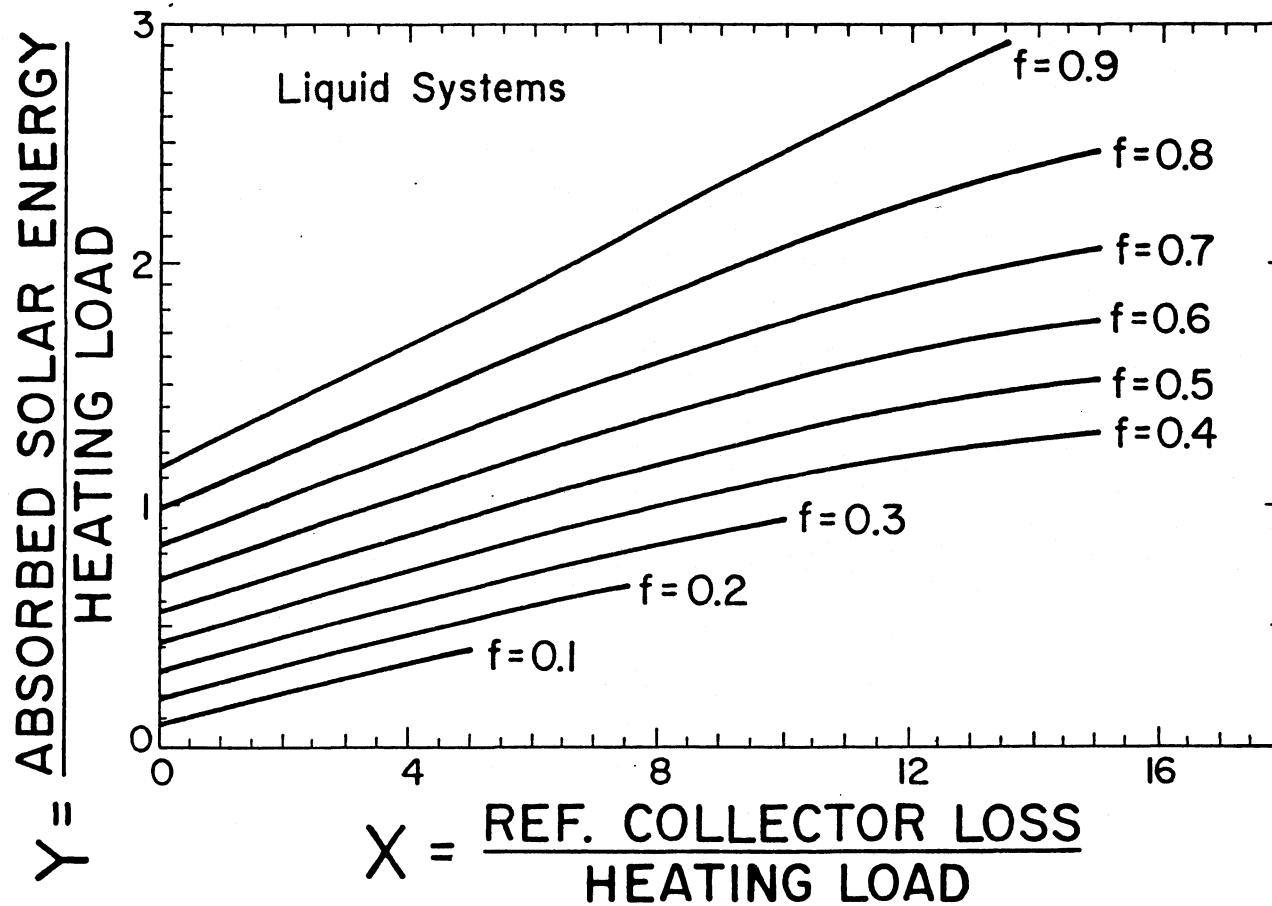
Figure 3.1   The f-Chart for Liquid Systems.   (Equation 3.8)
From Reference [4].

The X and Y parameter range which equation 3.3 is valid is shown in Figure 3.1 as the range of the constant solar fraction lines. Systems with high collector losses and low values of absorbed radiation will be outside of the limits of equation 3.3. Duffie and Beckman [12] recommend that these systems can be analyzed using the f-Chart method by extrapolating the constant solar fraction lines from Figure 3.1. Since these lines tend to be linear for low solar fractions and reasonably low values of the X parameter, a linear extrapolation algorithm was developed to be used for computer applications. For the X and Y parameter range given by

$$X < 12, \text{ and} \hspace{4cm} [3.4]$$

$$Y < 0.116 \cdot X - 0.128 \hspace{3cm} [3.5]$$

A linear extrapolation for the liquid f-Chart given by these limits is

$$f = 0.657 \cdot Y - 0.0321 \cdot X - 0.0009 \hspace{2cm} [3.6]$$

A number of assumptions were made in the derivation of the f-Chart method that restrict its applicability. The mains temperature must be between 5° and 20°C and the set temperature must be between 50° and 70°C. The design

method was derived for a preheat storage tank loss coefficient of 0.42 $W/m^2°C$ and an adiabatic auxiliary tank. Auxiliary tank loss coefficients greater than zero can be accounted for by adding the energy loss to the hot water load as shown by Buckles and Klein [6]. The assumed loss coefficient for the preheat tank is rather low. For example, the standard loss coefficient of a DHW tank from ASHRAE is 1.0 $W/m^2°C$ [33]. The f-Chart method will tend to overpredict the useful energy gain for systems with typical storage losses. Finally, the storage tanks were assumed to be fully-mixed, which occurs when the collector flowrate is high. The f-Chart method will as a result underpredict the solar fraction for thermally stratified storage systems.

A number of correction factors have been derived to modify either the X or Y parameter to increase the applicability of the f-Chart method. For liquid space heating systems, the f-Chart correlation was developed for a storage capacity per collector area of 75 ℓ/m^2. Variations in tank capacity can be accounted for by modifying the X parameter

$$\frac{X_c}{X} = \left[\frac{\text{actual storage capacity}}{75 \ \ell/m^2} \right]^{-0.25}$$ [3.7]

There is also a correction factor for liquid systems to

modify the Y parameter for variations in heat exchanger size.

The f-Chart method is an accurate tool for sizing SDHW systems with well-insulated tanks and high collector flowrates. A set of annual solar fractions from TRNSYS is compared with the f-Chart method in Figure 3.2. The simulations modeled the system shown in Figure 1.2, with a fully-mixed preheat tank and a preheat tank loss coefficient of 0.42 W/m^2°C. The design method compares to within 2.0% on an annual basis to simulation results. For thermally stratified storage the error is greater and highly biased, as shown in Figure 3.3. The collector inlet temperature for a thermally stratified preheat tank is lower than a fully-mixed preheat tank, decreasing collector losses and increasing performance. This causes the f-Chart method to underpredict the solar fraction from a stratified tank simulation, since the f-Chart method was developed for high-flowrate, fully-mixed tank solar systems.

This chapter will investigate a modification to the f-Chart method for systems that have a thermally stratified storage tank. The f-Chart design method presently has modifications to account for variations in heat exchanger size, storage size, pebble bed volume, and air flowrate. These alterations adjust the dimensionless X and Y
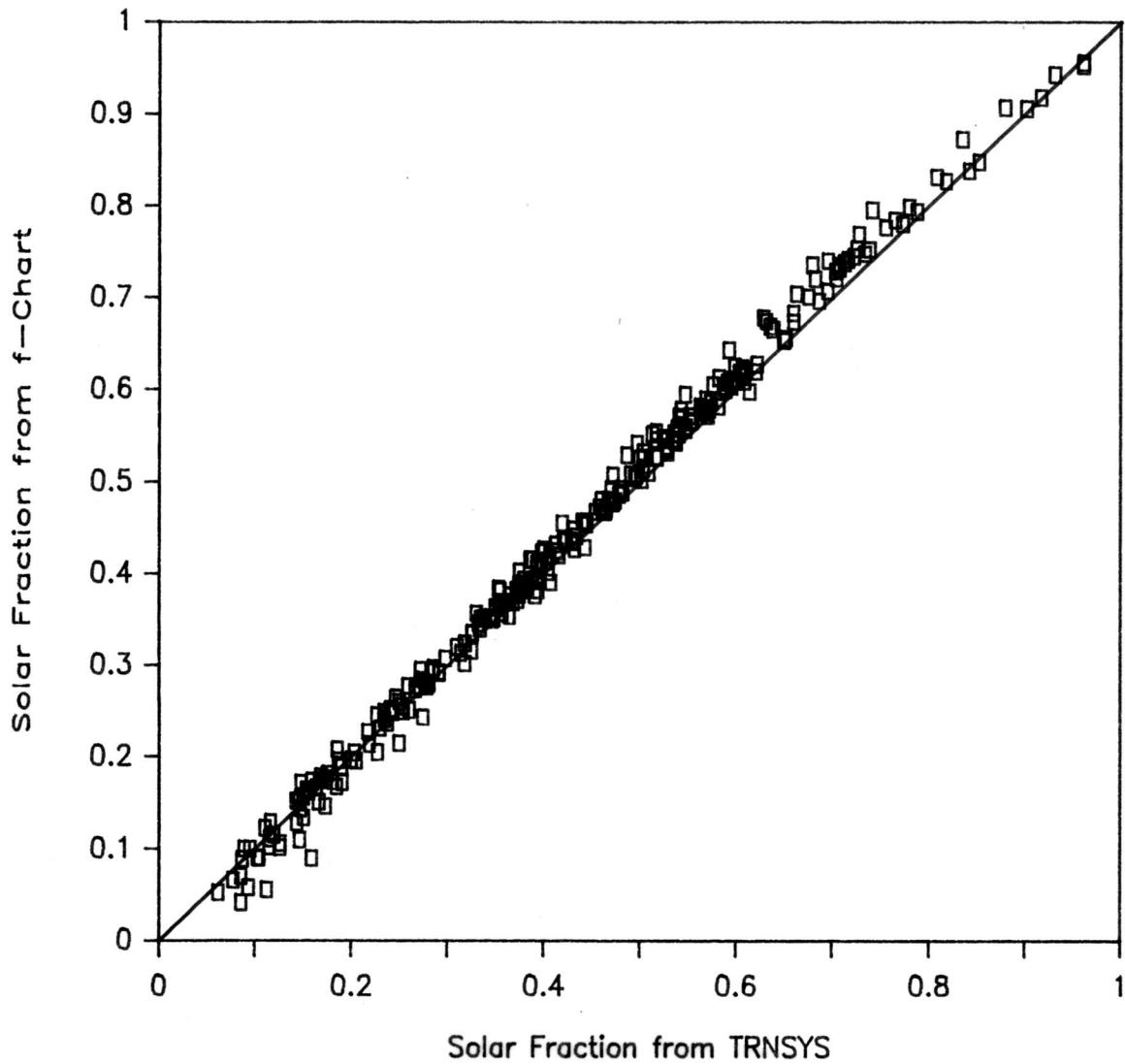
Figure 3.2   Annual Solar Fractions from TRNSYS Simulations with a Fully-Mixed Preheat Tank Compared to the f-Chart Method.
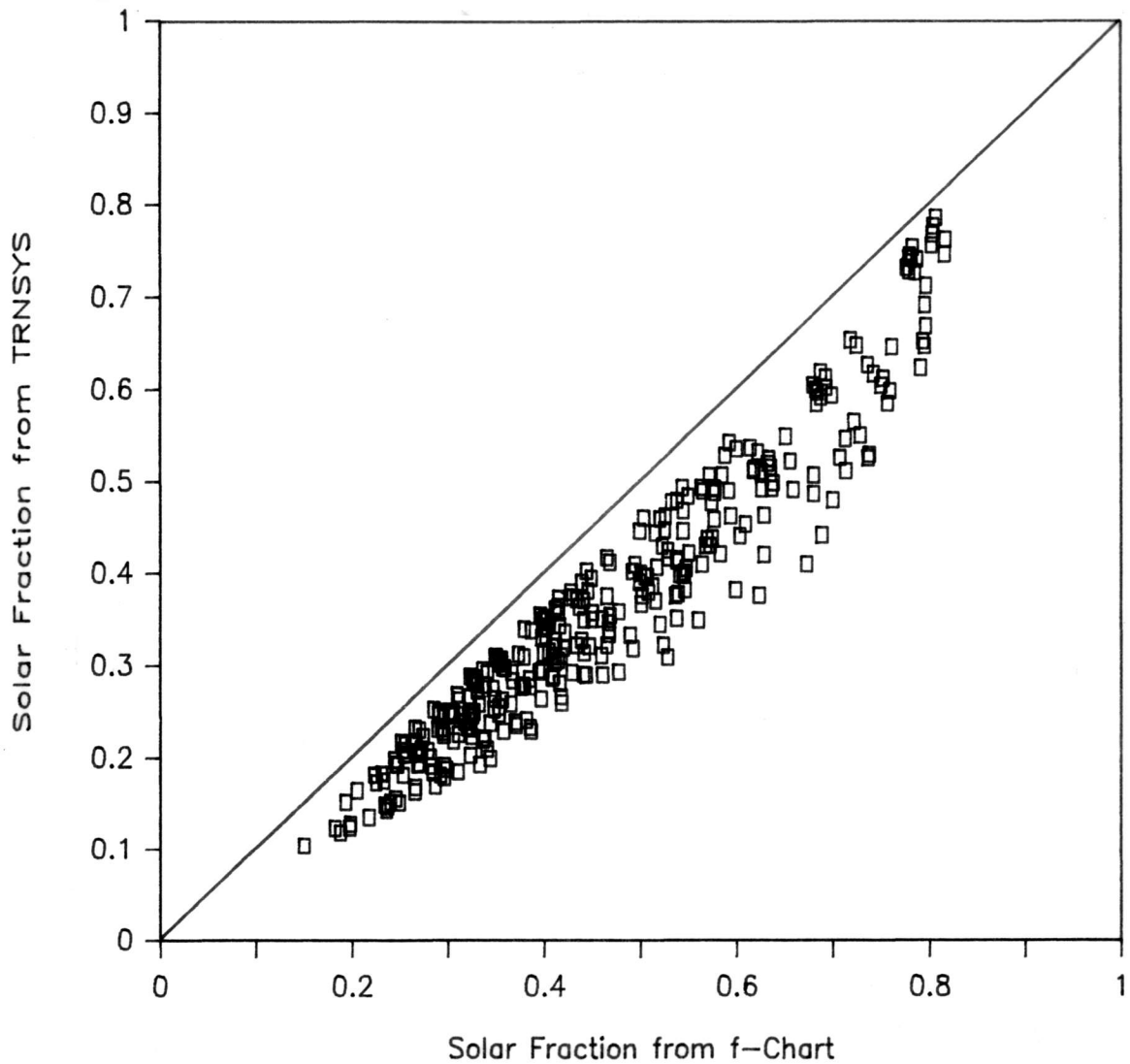
Figure 3.3   Annual Solar Fractions from TRNSYS Simulations
with a Stratified Preheat Tank Compared to the
f-Chart Method.

parameters. The air flowrate correction is needed to account for thermal stratification in the pebble bed and the dependence of F_R on flowrate. The air flow modification factor adjusts the X parameter.

A modification was attempted that decreased the X parameter for fluid tank stratification with the same equation form as the air flowrate correction. Reducing the air flowrate can increase system performance due to increasing the stratification in the pebble bed. The behavior of the X parameter was studied by obtaining the Y parameter from equation 3.2 and the solar fraction for a stratified tank from TRNSYS. The liquid system f-Chart equation for solar fraction was then solved for the X parameter. The results from the X parameter modification equation (i.e. using the form of the air flow modification) deviated from TRNSYS simulations by 8%. The data that had the highest error were the high and low collector flowrates. The air flowrate correction factor is limited to air flowrates less than 20 $\ell/s\text{-}m^2$ and greater than 5 $\ell/s\text{-}m^2$. This is a wide range for typical collector air flowrates, but the range of liquid flowrates presently being used is greater. A thermosyphon system, for example, may have a collector flow that is one-eighth the flowrate of an active system.

3.2 COLLECTOR AREA CORRECTION FACTOR

A correlation for thermally stratified storage was developed by employing the concept of the collector area ratio, A/A*. This quotient is the actual collector area divided by the area that a fully-mixed tank would require to achieve the same solar fraction that was obtained by a stratified system with the actual collector area, all else being the same. For example, a hypothetical solar domestic hot water set-up having a fully-mixed storage with a collector area of 4 m^2 produces a solar fraction of 43%. The same system operated at the same flowrate with a stratified storage tank yields a solar fraction of 51%. If the collector size needed by the mixed system to achieve a 51% solar fraction is 5 m^2, then the area ratio, A/A*, is 4/5 or 0.80.

A function was chosen so that at high flowrates, A/A* approaches unity as the tank storage tank becomes mixed; and a minimum value of A/A* (maximum difference between fully-mixed and stratified) occurs when the daily collector flow is approximately equal to the load flow, as observed by Wuestling and others [23-25]. The collector area ratio was also observed to be a function of the solar fraction.

A nonlinear regression analysis was employed to

minimize the RMS error between the TRNSYS simulations and the f-Chart method modified with A/A* function. The parameters used in the simulations were the base case system, three locations, 200 to 400 ℓ/day load flowrates, and 5 to 60 kg/hr·m^2 collector flowrates (Table 2.1). The resulting equation is:

$$A/A* = 1.-[3.53(\overline{M}_c/M_L)-1.71(\overline{M}_c/M_L)^2+0.655(\overline{M}_c/M_L)^3]$$
$$\exp[-1.15(\overline{M}_c/M_L)- 2.50f+0.047(\overline{M}_c/M_L)^2+2.17f^2] \quad [3.8]$$

where,

$\overline{M}_c/M_L$ the ratio of monthly-average daily collector flowrate to load flowrate from TRNSYS

f the monthly solar fraction for an equivalent system with a fully-mixed storage.

The solar fraction, f, appearing in the A/A* equation was for a mixed tank system, since the solar fraction from a stratified tank design would make the evaluation of A/A* iterative. The RMS error between TRNSYS and f-Chart utilizing equation 3.8 is 2.31% of annual solar fractions. The monthly error is 4.67% with a bias of 0.13%.

The equation for the collector area ratio as a function of mixed solar fraction and $\overline{M}_c/M_L$ is shown in Figure 3.4. Because of the nature of equation 3.8, values of $\overline{M}_c/M_L$ out of the range shown in Figure 3.4 should not be used.
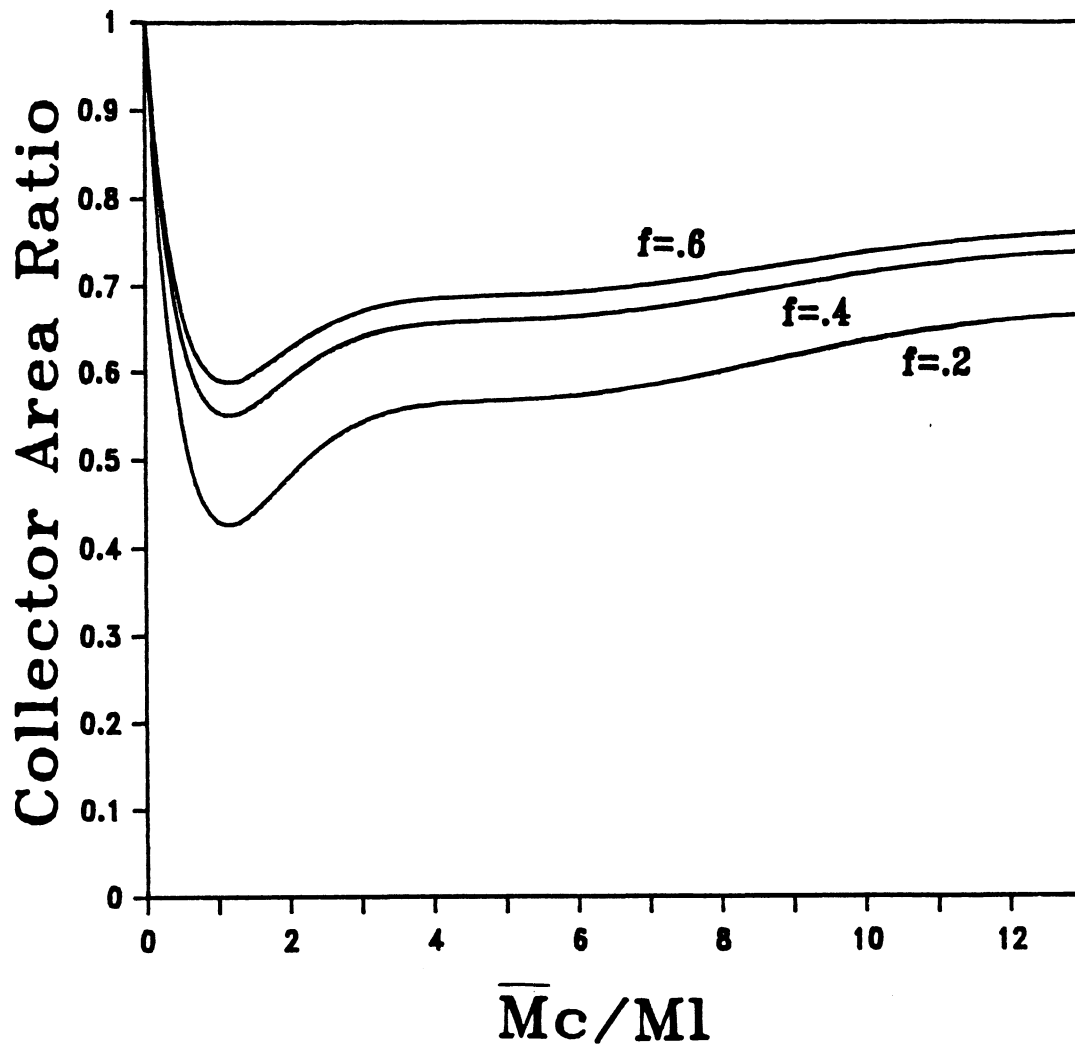
Figure 3.4   Collector Area Ratio Variation with the Ratio
of the Monthly- Average Daily Collector to Load
Flow and the Solar Fraction from a Mixed Tank
System.

Extrapolation can be done on the graph, or a fully-mixed tank assumed. The highest error was observed for months with a low clearness index. The f-Charts have been shown to underpredict in Seattle, WA [12] due to Seattle's low monthly solar radiation. A scatter plot of annual solar fractions from TRNSYS and the f-Charts using equation 3.8 appears in Figure 3.5.

The collector area correction factor was shown to agree well for the typical system for which it was developed, with $F_R(\tau\alpha)$ equal to 0.805 and $F_R U_L$ equal to 4.73 W/m^2°C. When systems with collectors having different performance characteristics were analyzed with the area correction method, the agreement with simulations was not as good. A system with an $F_R U_L$ value of 3.72 W/m^2°C was tested with the area correction factor method, giving an RMS error of 8%. The reason for this error can be seen in Figure 3.6. The modification will move along the line of varying collector area, as shown. The slope of this modification line is determined by the mixed-tank X and Y parameters. In general, moving up the collector area line will cause an increase in solar fraction, comparable to increasing the size of the solar collector.

The error of the area correction factor can be seen in the limit of zero collector loss coefficient. A stratified
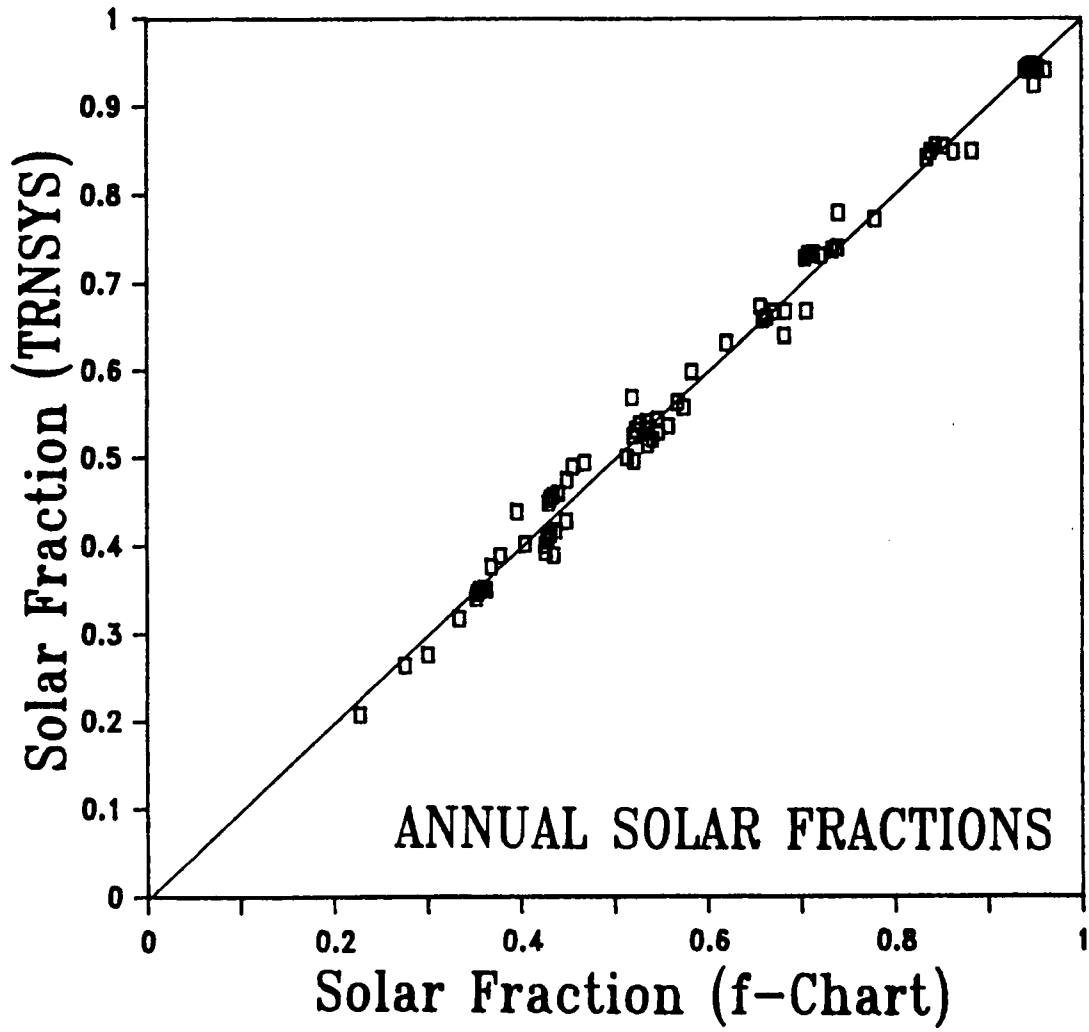
Figure 3.5   Comparison of the Stratified-Tank Annual Solar
Fractions from TRNSYS and the Annual Solar
Fractions from the f-Chart Method Modified with
Equation 3.1.
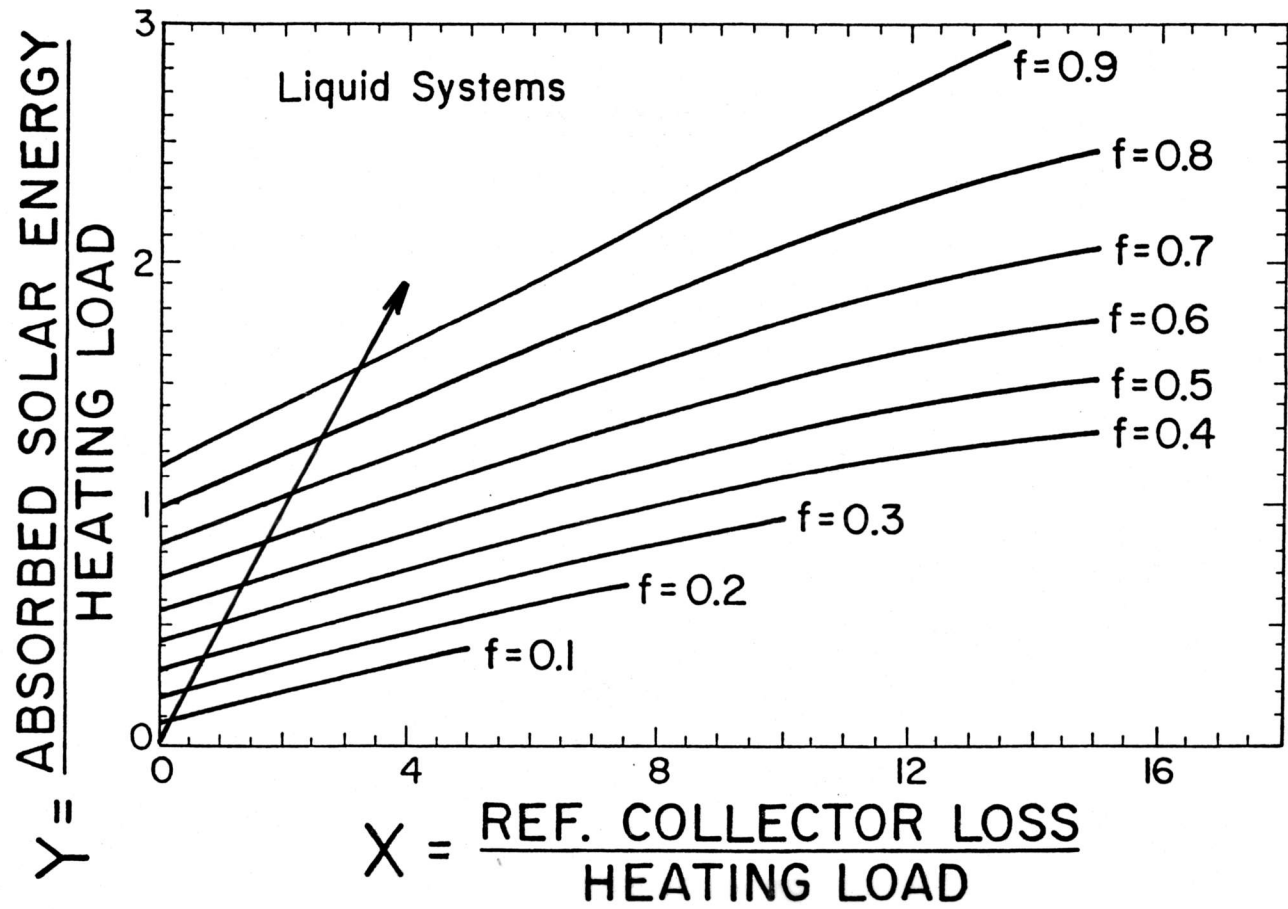
Figure 3.6   The Liquid System f-Chart with an Example of a
              Varying Collector Area Line.

and a mixed system that have collectors with no thermal
losses will perform identically, neglecting minor
differences in storage tank losses. The location on the f-
Chart of a collector with no losses lies on the ordinate,
and the area modification line is vertical. But for this
ideal system, the area correction factor will predict that
the stratified system will perform better than the mixed
system. For collectors with a loss coefficient close to
that of the system in the previous chapter, the area
modification correlation should give reasonable results.
The approach described in the next section was taken in
order to develop a stratification design method that could
be used with a wider range of collector types.

3.3 COLLECTOR LOSS COEFFICIENT CORRECTION FACTOR

The instantaneous performance of a solar collector is
given by

$$q_u = A_c F_R (\tau\alpha) I_t - A_c F_R U_L (T_i - T_a) \qquad [3.9]$$

The major reason that stratified systems perform better than
mixed tank systems is the temperature reduction of the fluid
flowing into the collector. The first term on the right
hand side is the absorbed energy, and the second is the

energy lost by the collector. The area correction factor modified A_c to account for an increase in the useful energy. But for a a collector with no thermal losses, increasing the collector area to account for stratification implies that a stratified system is causing greater solar absorption, which is incorrect. Stratification increases the useful energy gain of a system by decreasing losses, i.e., decreasing the second term of the Hottel-Whillier equation. Modifying the collector loss coefficient, U_L, is a method by which the increase in useful energy caused by stratification can be correlated and behave correctly in the extremes of the parameters.

3.3.1 Collector Loss Coefficient Methodology

The f-Charts were developed assuming the preheat tank to be fully-mixed. A modification is needed to have the f-Charts predict the performance of SDHW systems having stratified preheat storage. The solar fraction from a stratified system can be obtained by an otherwise identical system with a fully-mixed tank and a lower collector loss coefficient. For example, if a stratified SDHW design obtained a solar fraction of 55%, and a mixing device is installed in the preheat tank the solar fraction will be

reduced. However, it can again be raised to 55% solar fraction if the collector back and side losses were reduced by adding more insulation.

The collector heat removal factor is a function of the collector loss coefficient. The variation of F_R with U_L is shown in Figure 3.7. This figure shows that a a collector with no thermal losses has a heat removal factor of one and increasing the loss coefficient causes the heat removal factor to approach zero asymptotically. The heat removal factor is a complicated function of the collector loss coefficient. A stratification modification to the f-Chart method that is based on the collector loss coefficient will also modify F_R.

The f-Chart method includes the collector losses in the X parameter, and the heat removal factor in both parameters. Figure 3.8 is an expanded view of a liquid f-Chart. The dashed line on this figure is the path taken by decreasing collector losses, while simultaneously modifying the heat removal factor. The bottom point is the location on the liquid f-Chart of a mixed tank system. The mixed tank solar fraction can be obtained from the original f-Chart method with coordinates X_{mix} and Y_{mix}. If the collector has no thermal losses, then its X parameter would be zero, and the Y parameter would be equal to the ratio of the absorbed
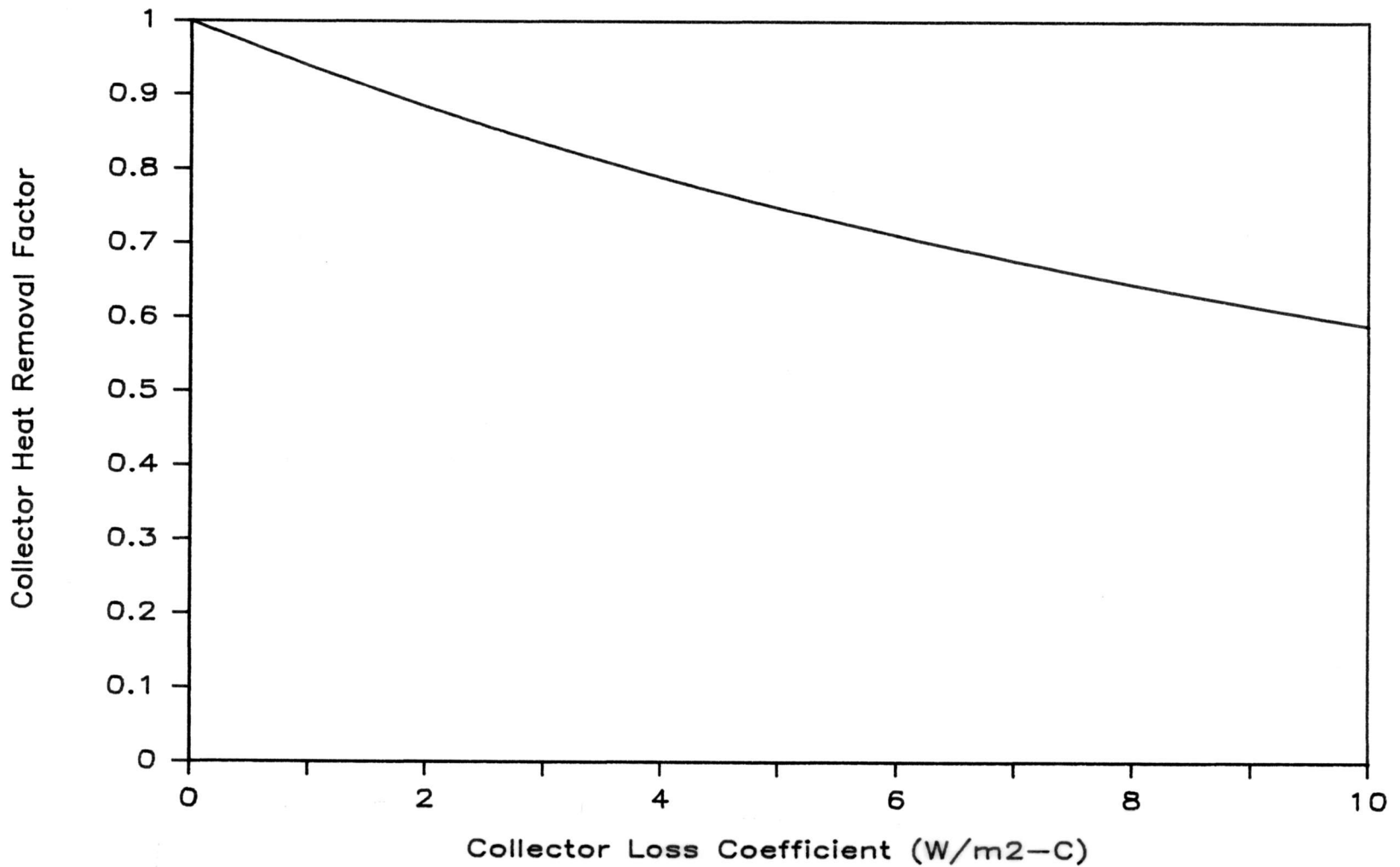
Figure 3.7   The Relationship Between the Collector Heat Removal Factor and the Collector Loss Coefficient. A_c = 4.2m^2, M_c = 10 kg/hr-m^2, h=300W/m^2°C, W = 0.15 m, d_i = 0.009 m, d_o = 0.01, δ_p = 0.001.
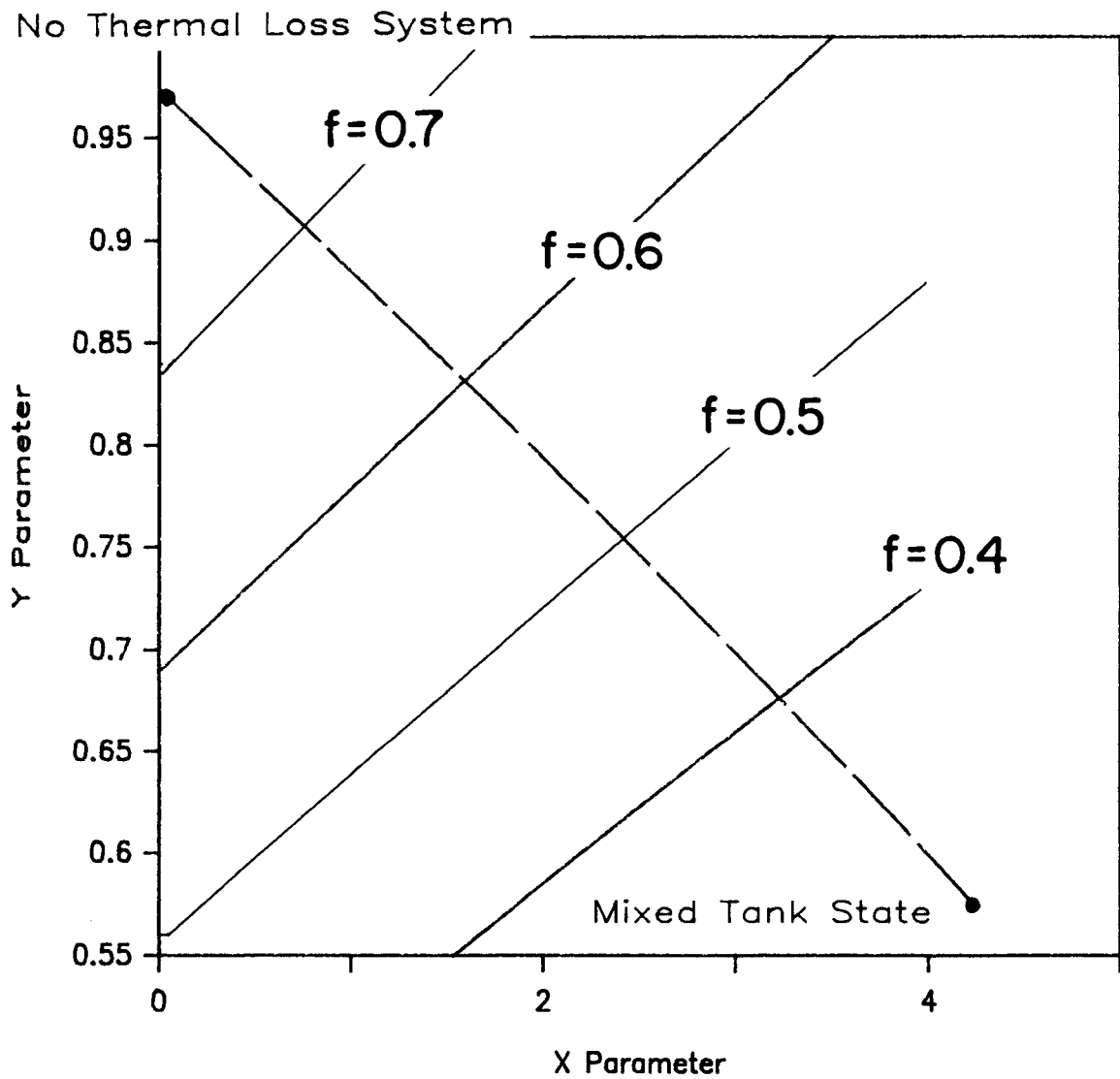
Figure 3.8   The Variation of the X and Y Parameters on a Liquid System f-Chart Caused by Increasing U_L and Correspondingly Decreasing F_R.

radiation to the load, given by

$$Y_{max} = A_c (\overline{\tau\alpha}) \bar{H}_T N / L.$$ [3.10]

The upper point on the varying U_L line in Figure 3.8 is the location on the f-Chart of a system that has no thermal losses. The stratified tank solar fraction will always be between the limits obtained for a fully-mixed system with the correct collector loss coefficient and a collector with no thermal losses. The curved line connecting the maximum and the mixed solar fraction is that which would be obtained if the collector loss coefficient were varied from the original value to zero, and correspondingly the heat removal factor was varied from the original value to one. The slight curve in this line is due to the relationship between F_R and U_L.

The equation relating the collector heat removal factor to the collector loss coefficient (Figure 3.7) is unnecessarily complex for the accuracy warranted for use in a design method. If the path shown in Figure 3.8 is approximated as being linear, then a computationally simple relationship can be established between the maximum, stratified, and mixed performances, shown in Figure 3.9. In this figure, the maximum and mixed X and Y parameters are shown as before. The stratified performance is constrained
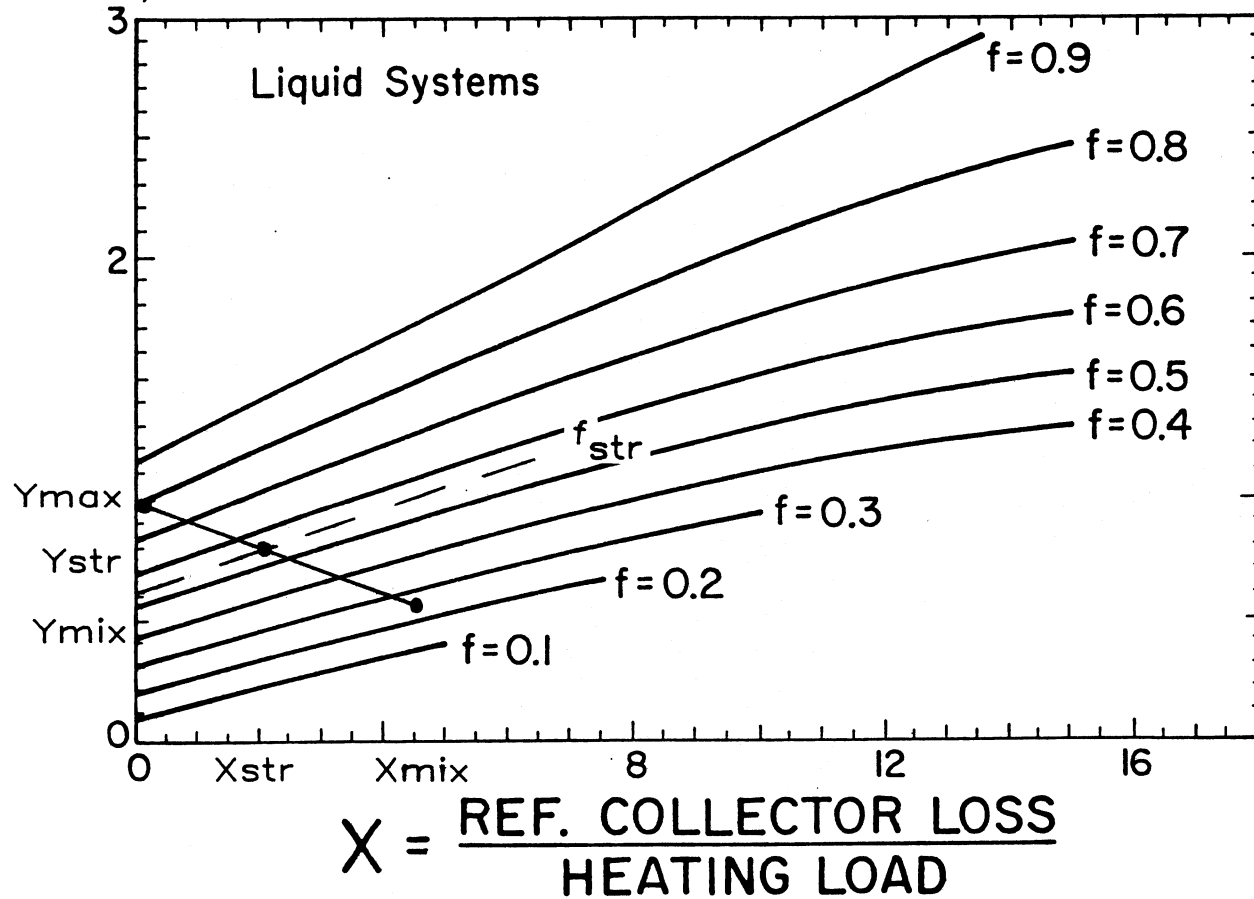
Figure 3.9   The Relationship Between the f-Chart Parameters
for a Collector with no Thermal Losses, a
System with a Fully-Mixed Storage, and a System
with a Stratified Storage.

as being colinear on a line between the maximum and mixed values. Using similar triangles, a relationship between the three sets of f-Chart parameters can be expressed as

$$\frac{\Delta X}{\Delta X_{max}} = \frac{X_{mix} - X_{str}}{X_{mix}} \qquad [3.11]$$

$$= \frac{Y_{str} - Y_{mix}}{Y_{max} - Y_{mix}} \qquad [3.12]$$

The mixed X and Y parameters can be obtained from the original f-Chart and Y_{max} can be found from equation 3.10. If an equation for the $\Delta X / \Delta X_{max}$ is known, then the stratified X and Y parameters can be calculated from equations 3.4 and 3.5, yielding the stratified solar fraction when they are used in the f-Chart method.

3.3.2 Results

The relationship between $\Delta X / \Delta X_{max}$ and the monthly-average collector to load flow, $\overline{M}_c / M_L$, was investigated. A computer program was written to determine $\Delta X / \Delta X_{max}$, using simulation data for Madison, Albuquerque, and Seattle with collector flowrates ranging from 2.5 to 60 kg/hr-m^2 and daily load flows ranging from 200 to 400 ℓ/day. The program calculated the collector heat removal factor

analytically [12], and solved for the mixed and maximum f-Chart parameters. The stratified system X and Y parameters are constrained by being on a line between the mixed-tank and maximum f-Chart parameters. In this computer program, the stratified tank X and Y parameters are then obtained from colinearity and the stratified-tank simulation solar fractions. A set of points from this program is shown in Figure 3.10.

A general relationship between $\Delta X / \Delta X_{max}$ and $\overline{M}_c / M_L$ can be seen in Figure 3.10 . The largest values of $\Delta X / \Delta X_{max}$ are the points where the performance difference between the stratified system and the mixed system is greatest. This maximum occurs when the daily collector flowrate is about equal to the daily load flow, as shown by Wuestling, et al. [22]. As the collector to load flow ratio increases, the performance of the mixed and stratified tank systems approach each other since the temperature difference between the top and bottom of the stratified tank is decreasing due to recirculation. The heat removal factor becomes small and $\Delta X / \Delta X_{max}$ approaches zero as the flowrate approaches zero. The limits on $\Delta X / \Delta X_{max}$ are one and zero. The upper limit is approached for high solar fractions and low recirculation rates, where the collector inlet temperature is close to the mains water, and the system acts
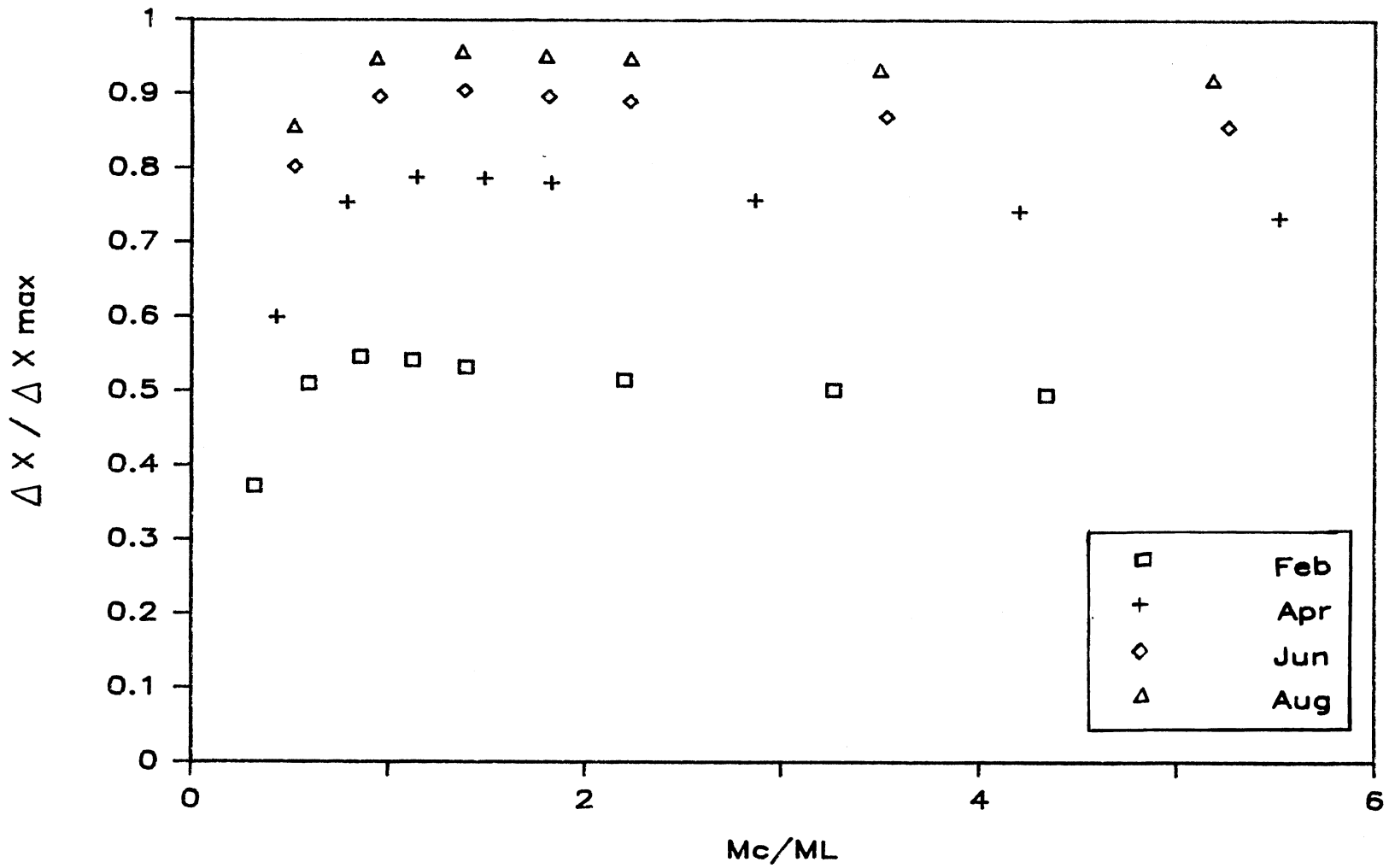
Figure **3.10**   Simulation Results of ΔX/ΔXmax Versus Mc/ML
for **Madison**, 200 ℓ/day Load, and the **Base Case**
System.

as if the mains water is connected directly to the collector inlet ("once-through" design).

The ratio $\Delta X / \Delta X_{max}$ is a function of the collector to load flow ratio and solar fraction. An equation that exhibits the behavior discussed in the previous paragraph is of the form $X(X^2 + 1.)$ Other formulae that can fit the above criteria include $X \cdot exp(-X)$. This equation was investigated, but it produced higher residuals and consequently a higher RMS error. The exponential equation did not follow the simulations near the peak causing a biased error for points with collector to load flow ratios near one. Both of these functions will not follow simulation results for very low collector flowrates. The equation will overpredict $\Delta X / \Delta X_{max}$ for low values of $\overline{M}_c / M_L$. There are equations that would better follow these low flowrates, such as the beta function, but their complexity does not lend itself to design methods, and very low collector flowrates are not a desirable operating region.

A nonlinear regression routine was used to find the coefficients that minimized the RMS error between TRNSYS simulations and the f-Chart method modified with the stratification correction formula. The utilizability correlation from Evans, et al. [13] was used to calculate $\overline{M}_c / M_L$ for the f-Chart stratification modification since it

is computationally easier to solve. The X parameter

modification, $\Delta X / \Delta X_{max}$, is

$$\frac{\Delta X}{\Delta X_{max}} = \frac{C1 \; M}{[C2 \; M + C3 \; f + C4 \; f^2]^2 + 1.} \qquad [3.13]$$

where,

C1, C2, C3, C4 are coefficients from the

regression routine,

f   the solar fraction from a mixed

storage system, and

M   a correlation for the collector to load flow

The solar fraction from a stratified system was tried in

place of the mixed solar fraction, and although the RMS was

about the same, using the stratified solar fraction would

have involved iteration. The RMS error with all of the data

was 3.74% annually and 5.55% monthly with a bias of 0.63%.

The data that exhibited a high error included the very

low collector flowrates, 2.5 - 7.5 kg/hr·m^2. The form of

the equation used to correlate the $\Delta X / \Delta X_{max}$ does not fit

well at very low flowrates. The equation form of equation

3.13 was chosen due to its computational simplicity and its

behavior at low flow or conventional flowrates. The

flowrates in error all have a collector to load flow of less

than one, indicating that they are operating at an

undesirable collector to load ratio. Equation 3.13 is

asymptotic to a line of slope one and origin intercept (Y = X) as M approaches zero. The actual data is asymptotic to a line of slope zero (Y = 0). Over the range of collector to load flows, the correction is good, but it is strongly biased with high relative error for very low collector flows, as shown in Figure 3.11 . If only the range of flowrates from 10 - 60 $kg/hr \cdot m^2$ is considered, the annual RMS error is 3.15%, the monthly error is 5.49%, and the bias is 0.54%. High residuals were also noted for Seattle. The f-Chart method tends to underpredict for this location. This is due to Seattle's relatively low solar radiation in the winter and high utilizability.

The set of coefficients that gave the lowest RMS error for all of the locations to be used in equation 3.13 is:

C1 = 1.040

C2 = 0.726

C3 = 1.564

C4 = -2.760 .

Equation 3.13 with the these coefficients is plotted in Figure 3.12 . Because of the nature of equation 3.13, a high solar fraction combined with a collector to load flow ratio near one can give $\Delta X / \Delta X_{max}$ greater than one. For these cases, $\Delta X / \Delta X_{max}$ should be set equal to one. A plot of annual solar fractions from simulation results and the f-
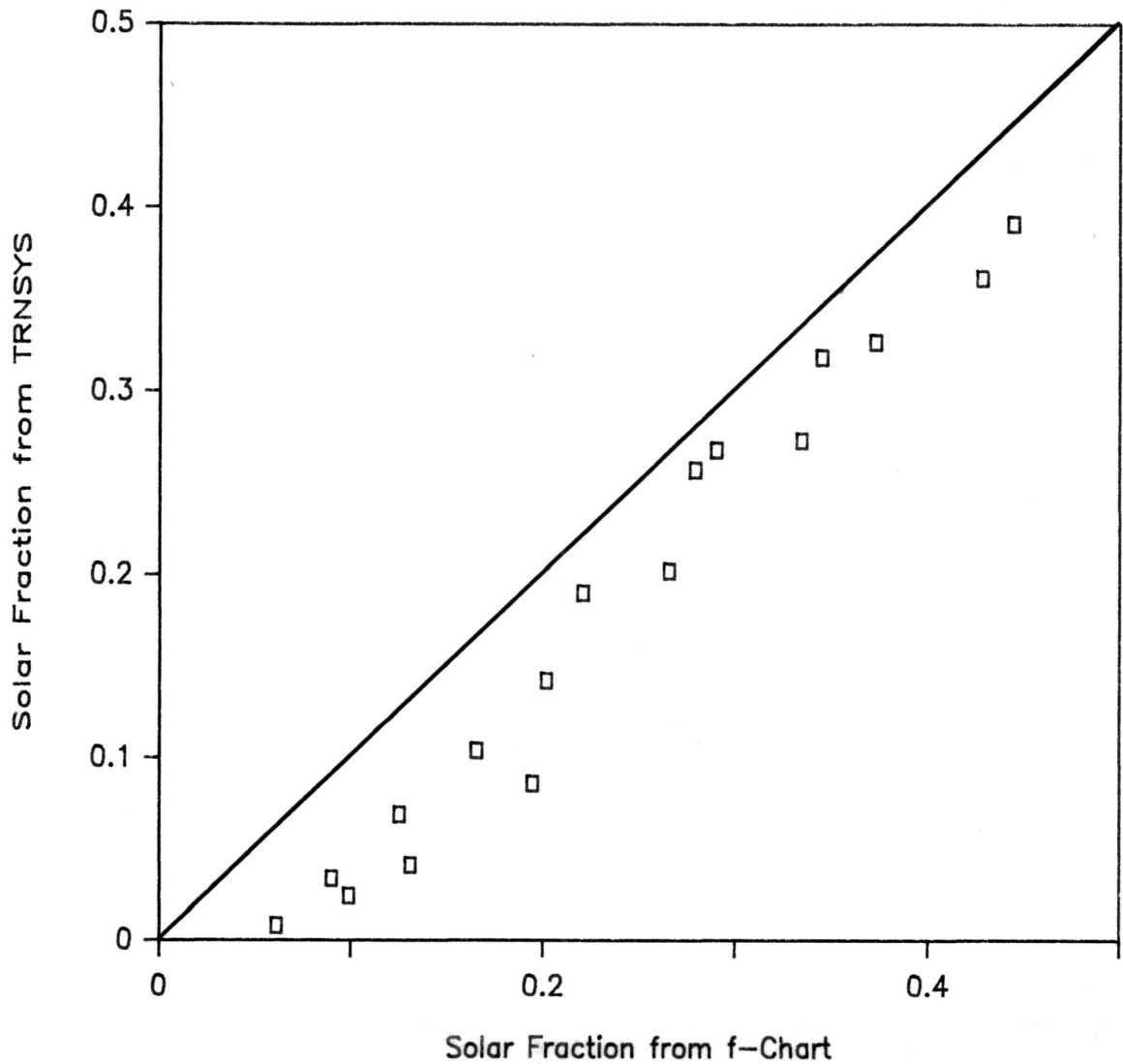
Figure 3.11 Annual Solar Fractions from TRNSYS Simulations Versus the f-Chart Method Modified with the Stratification Correction for $\bar{M}_c/M_L$ less than 0.3
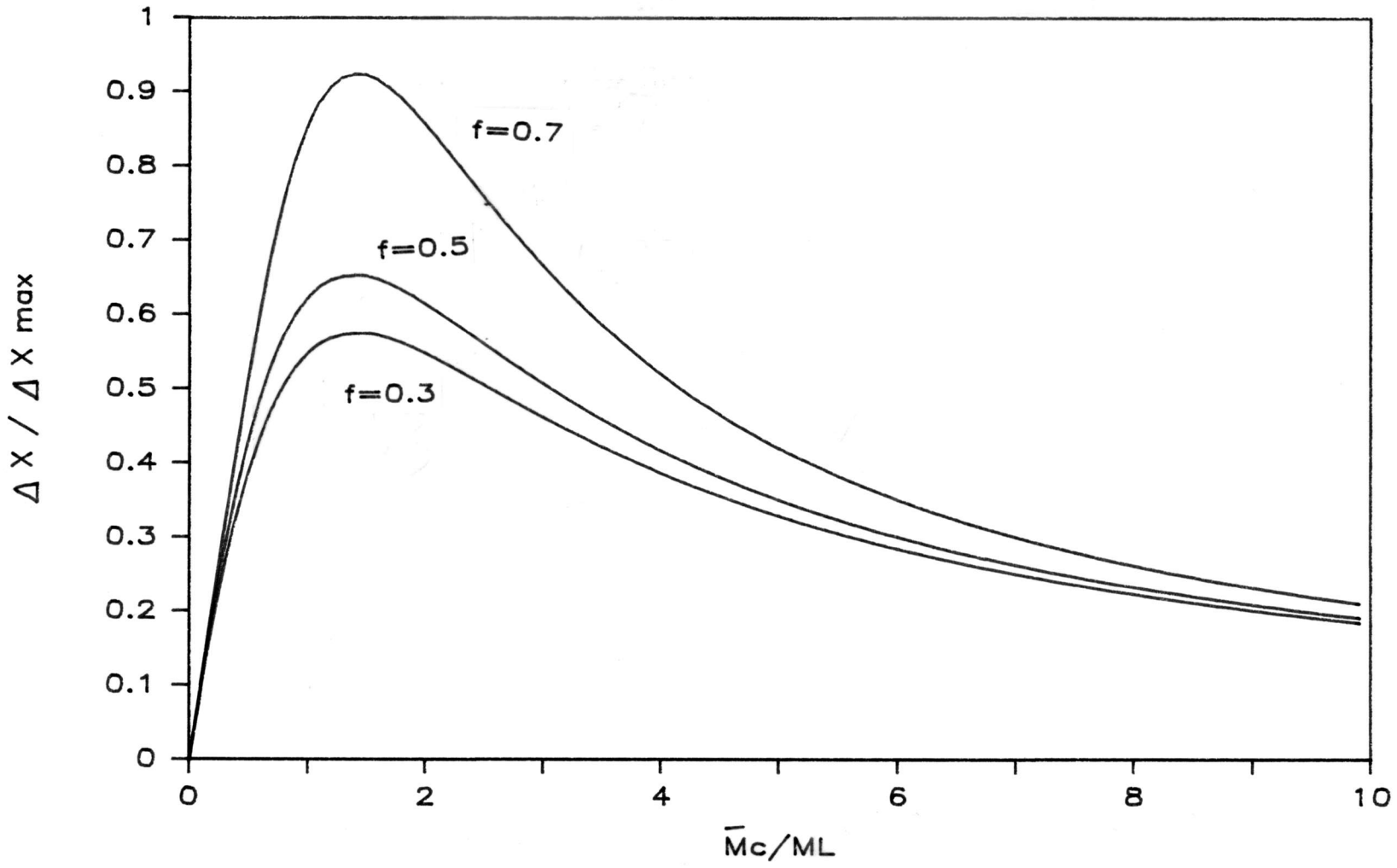
Figure 3.12 ΔX/ΔXmax for the f-Chart method

Chart method corrected for stratified storage is shown in Figure 3.13 .

3.4 EXAMPLE

As an example of using the f-Chart method modified for stratified storage, a low-flow system located in Madison will be analyzed for the month of June. Meteorological data and design parameters are listed in Table 3.1 . The first step in the procedure is obtaining a value for the solar fraction of a mixed system to be used in Equations 3.7. The f-Chart method is employed using the actual collector loss coefficient, giving an X parameter of 2.59, a Y parameter of 0.77, and a solar fraction of 50.2%. The monthly-average daily collector to load flow ratio can be evaluated by equation 3.5, and it is found to be 1.40 . From Figure 3.12, or equation 3.13, $\Delta X / \Delta X_{max}$ is equal to 0.632 . Going back to the f-Chart method with an X parameter of 2.59(1-0.632) or 0.954 and a Y parameter of 0.942, the solar fraction for a stratified system is found to be 71.9%.
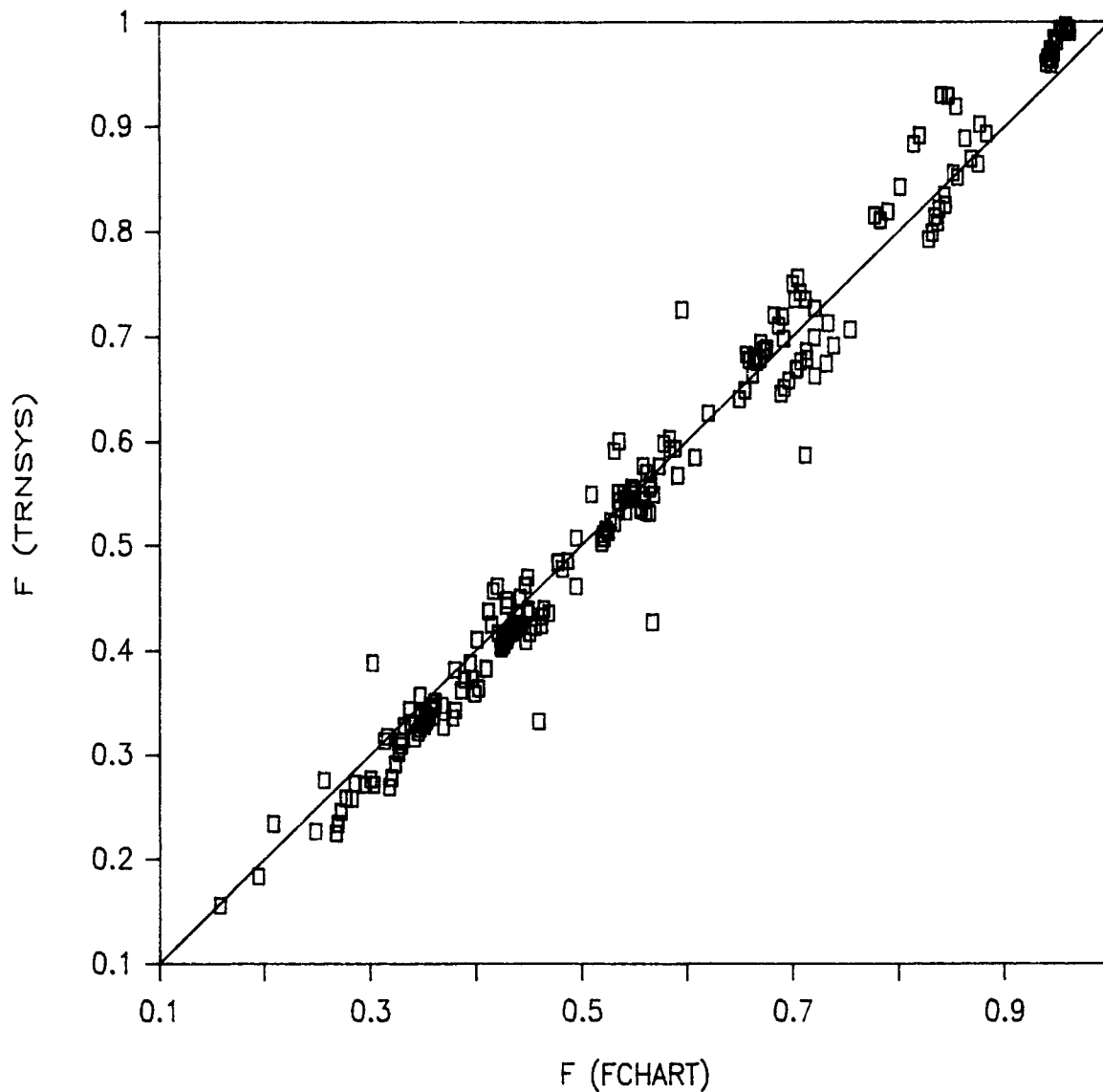
Figure **3.13** Annual Solar Fractions from TRNSYS Simulations
Versus the f-Chart Method Modified with the
Stratification Correction, for $\dot{M}c=10\text{-}60$ kg/hrm2
and all Locations, Loads, and Systems.

Table 3.1 Parameter Values for System in f-Chart Example

Location	Madison, Wisconsin
Meteorological	June
	$\bar{H}$=17.07 MJ/m^2
	T_a=19.6° C
	$\bar{K}_t$=.513
Collectors	A_c=4.2 m^2
	$F_R(\tau\alpha)_n$=0.805
	$\overline{(\tau\alpha)}/(\tau\alpha)/_n$=.925
	$(\tau\alpha)$=.913
	$F_R U_L$=4.73 W/m^{2}C
	$\dot{M}_c$(test)=71.5 kg/hr m^2
	$\dot{M}_c$(use)=10 kg/hr m^2
	slope=latitude=43.1°
Preheat Tank	Volume=0.30 m^3
	Height=1.5 m
	U=0.42 W/m^{2}C
Auxiliary Tank	negligible losses
Hot Water Load	Demand=300 ℓ/day
	T_m=10 C
	T_w=60 C
	T_∞=20 C

CHAPTER FOUR: MODIFICATION TO THE $\bar{\phi}$,F-CHART METHOD
FOR THERMALLY STRATIFIED SDHW SYSTEMS

4.1 THE $\bar{\phi}$,f-CHART METHOD

The f-Chart method is a design tool for systems with the restrictions discussed in the previous chapter. The utilizability method is useful for systems with a known critical level. Another design method was created which combines aspects of both of these design methods and has fewer restrictions. The $\bar{\phi}$,f-Chart method [5] was originally developed for closed-loop solar systems shown in Figure 1.3. Braun, et al. [34] has extended the $\bar{\phi}$,f-Chart method to open-loop designs, such as the standard SDHW system shown in Figure 1.2 . These designs have mass exchange between the load and storage. Open-loop systems have a load that is characterized by two temperatures, the mains water temperature and the set temperature. Auxiliary energy is supplied if the delivery temperature from the storage is less than the set temperature.

The method for estimating the solar fraction of open-loop systems by the $\bar{\phi}$,f-Chart method is as follows. The useful energy for a solar system is given by

$$Q_u = Q_{max} - a(e^{bf}-1.)\,(1.-e^{cX})\,(e^{dZ})L \qquad [4.1]$$

where,

$$Q_{max} = \overline{\phi}_{max} A_c F_R (\overline{\tau\alpha}) \overline{H}_t N$$

$$a = 0.015 \left[\frac{M_t C_P / A_c}{350. kJ/m^2 °C} \right]^{-0.76}$$

$$b = 3.85$$

$$c = -0.15$$

$$d = -1.959$$

$$X = A_c F_R U_L (100°C) \Delta\tau / L$$

$$Z = L / (M_L C_p (100°C))$$

M_t mass of fluid in the preheat tank

M_L monthly mass of fluid removed from the system

       by the hot water demand

L   monthly energy removed from the system

       by the hot water demand

The term $\overline{\phi}_{max}$ is the utilizability function evaluated at the monthly - average delivery temperature, T_d. The monthly average delivery temperature is the average temperature of the fluid going from the preheat tank to the auxiliary tank. The second part of equation 4.1 corrects for the fact that the inlet temperature is not always equal to T_d. The dimensionless parameter, Z, is important for systems that have set temperatures significantly higher than T_d, such as domestic hot water designs.

An equation for the storage losses is

$$Q_{LS} = (UA)_{tank}(T_{tank} - T_{env}) \qquad [4.2]$$

Storage losses are evaluated at the average tank temperature. A correlation for the average tank temperature, T_{tank}, to be used in equation 4.2 has been determined by Braun, et al. to be

$$T_{tank} = T_d + g(e^{kf} - 1.)(e^{hZ}) \qquad [4.3]$$

where,

$$g = 0.2136 \left[\frac{M_t C_p / A_c}{350. \, kJ/m^2 \, {}^\circ C} \right]^{-0.704}$$
$$h = -4.002$$
$$k = 4.702.$$

The energy supplied from solar to the load, Q_S, is the minimum of the load and the delivered energy

$$Q_S = min[M_L C_p (T_d - T_{main}), L] \qquad [4.4]$$

The solar fraction employed in this study, as discussed in section 1.2.1, is the ratio of the supplied energy to the hot water load

$$f = \frac{Q_S}{L} \qquad [4.5]$$

A monthly energy balance on the SDHW system, assuming that

the change in storage internal energy is negligible is given by

$$Q_U - Q_{LS} - Q_S = 0.$$ [4.6]

TRNSYS simulations of DHW systems indicate that the monthly change in storage internal energy is less than ±1% of the useful energy, for systems having typical storage volumes.

The open-loop $\bar{\phi}$,f-Chart method involves an iterative solution of equations 4.1 to 4.6 for T_d. For monthly simulations, an approximate initial value for T_d is the solution from the previous month.

Similar to the f-Chart method, the $\bar{\phi}$,f-Chart design tool is accurate for predicting the performance of SDHW systems with a fully-mixed storage tank. It also assumes fully-mixed storage, hence it will underpredict the solar fraction for a system that has a thermally stratified storage tank.

4.2 CORRECTION FACTOR METHODOLOGY

The correction to the $\bar{\phi}$,f-Chart method for stratified storage was similar to the modification used for the f-Chart method. A correlation for $\Delta X/\Delta X_{max}$ was obtained in the f-Chart correction. The $\Delta X/\Delta X_{max}$ modifies the collector

loss coefficient a proportionate amount. As shown with the f-Chart correction, the heat removal factor also is modified so that the stratified state is colinear on the liquid f-Chart between the maximum absorbed radiation and the mixed state. For the $\bar{\phi}$,f-Charts this ratio reduces to

$$\frac{\Delta X}{\Delta X_{max}} = \frac{X_{mix} - X_{str}}{X_{mix}}$$

$$= \frac{(F_R U_L)_{mix} - (F_R U_L)_{str}}{(F_R U_L)_{mix}} \qquad [4.7]$$

This equation can be solved for $F_R U_L$ for a stratified storage system as

$$(F_R U_L)_{str} = (F_R U_L)_{mix} (1.- \frac{\Delta X}{\Delta X_{max}}) \qquad [4.8]$$

From the f-Chart correction, it was shown that

$$\frac{\Delta X}{\Delta X_{max}} = \frac{Y_{str} - Y_{mix}}{Y_{max} - Y_{mix}}. \qquad [4.9]$$

Substituting the definition of the Y parameter into equation 4.9 and solving for the stratified heat removal factor yields

$$(F_R)_{str} = \frac{\Delta X}{\Delta X_{max}} + (1.- \frac{\Delta X}{\Delta X_{max}}) \ (F_R)_{mix} \qquad [4.10]$$

Equations 4.8 and 4.10 can be used in the $\overline{\phi}$,f-Chart design method once a relationship for the $\Delta X/\Delta X_{max}$ equation is determined. The form of $\Delta X/\Delta X_{max}$ is similar to that used in the original f-Chart method. The equation is a function of collector to load flow ratio and solar fraction, it intersects the origin, has a maximum at an $\overline{M}_c/M_L$ value of about one, and is asymptotic to the abcissa at high collector to load flow ratios.

4.3 RESULTS

A nonlinear regression package that utilizes a gradient search method was employed to minimize the sum of the squares between TRNSYS simulations and the $\overline{\phi}$,f-Chart method modified with a stratification correction. The form of the $\Delta X/\Delta X_{max}$ equation is similar to that used in the f-Chart stratified tank correction

$$\frac{\Delta X}{\Delta X_{max}} = \frac{C1 \ M}{[C2 \ M + C3 \ f]^2 + 1.} \qquad [4.11]$$

where,

C1, C2, C3 coefficients from the regression routine,

f_m the solar fraction from a mixed storage system, and

M   a correlation for the collector to load flow

The collector operating time was evaluated by using a correlation for the monthly-average daily utilizability developed by Klein [11]. As mentioned before, this equation is more computionally involved than Evans' correlation, but more accurate over a wide range of critical radiation levels. A program that impliments the $\overline{\phi}$,f-Chart method, such as F-CHART4.1, requires the evaluation of the variables in equation 1.16. For these programs, evaluation of equation 1.16 is not difficult, since most of the input variables are previously calculated.

The same range of parameters used in the f-Chart method were used here; three locations, three systems, three locations, ten flowrates and twelve months, for a total of 3240 pieces of data. The initial run used the day and night ambient temperature in the critical level equation and Evans' utilizability correlation for collector operating time equation. The RMS error was 2.64% annually and 3.93% monthly, with a bias of 0.29%.

When Erbs' daytime ambient temperature equation 1.20 was used, no change in the errors were observed. This

indicates that using the average day and night ambient temperature in evaluating the critical level is a good approxmation. The negligible difference in the utilizability evaluated with the ambient or the daylight temperature is consistent with findings from Reference [13].

If Mitchell's collector operating time equation is used to estimate the collector to load flow ratio, the error decreases negligibly to 2.60% annually, 3.88% monthly, and a bias of 0.21%. This would indicate that the solar fraction obtained from the $\overline{\phi}$,f-Chart method modified with equation 4.11 is relatively insensitive to the accuracy of the pump-on time equation as long as the general relationship is correct. This is caused by the nature of $\Delta X / \Delta X_{max}$ curve. The slope of the difference between a stratified and mixed system, and consequently $\Delta X / \Delta X_{max}$, is small at high values of the collector to load flow ratio. The error caused by using the mains water temperature in the critical level evaluation is reduced due the insensitivity of the $\Delta X / \Delta X_{max}$ relationship to flowrate at high collector to load flow ratios. The collector flowrates used in the TRNSYS simulations cover a wide range, with most of them occuring in the region where the slope is small, explaining the negligible difference between the two collector operating time equations.

As discussed previously, the very low collector flowrates caused a bias error due the the form of the equation. The error without these very low flows are listed in Table 4.1. The annual RMS error for the flowrates 10-60 kg/hr·m^2 is only 2.07%, with no bias. The bias was eliminated since the $\Delta X/\Delta X_{max}$ tends to overpredict solar fraction at the very low flowrates. The range of collector flowrates 10-60 kg/hr·m^2 cover a typical low-flow control strategy operating range. The coefficients for equation 4.11 that yielded the lowest monthly RMS error are:

$C1 = 0.6078$

$C2 = 0.6019$

$C3 = -0.1657$

$\Delta X/\Delta X_{max}$ from Equation 4.11 is plotted versus the collector to load flow ratio in Figure 4.1 .

A comparison of TRNSYS simulation results and annual solar fractions from the $\overline{\phi}$,f-Chart method modified with equation 4.11 is shown in Figure 4.2 . The difference between the design method and simulations is reasonably small. The three points with the highest RMS error in Figure 4.2 were for Seattle with the high quality collector system. Locations with a very low $\overline{K}_t$ have generally shown the largest error in previous design methods. Overall, the modification to the $\overline{\phi}$,f,Chart method for systems with a

Table 4.1 The Error of the Stratified Design Method for Varying Ranges of Collector Flowrate

Collector Flowrates ($kg/hr \cdot m^2$)	RMS Error (%) Annual	Monthly	Bias (%)
2.5, 5, 7.5, 10, 12.5, 20, 30, 40, 50, 60	2.60	3.93	0.27
5, 7.5, 10, 12.5, 20, 30, 40, 50, 60	2.55	3.89	0.24
7.5, 10, 12.5, 20, 30, 40, 50, 60	2.51	3.81	0.18
10, 12.5, 20, 30, 40, 50, 60	2.07	3.45	0.03
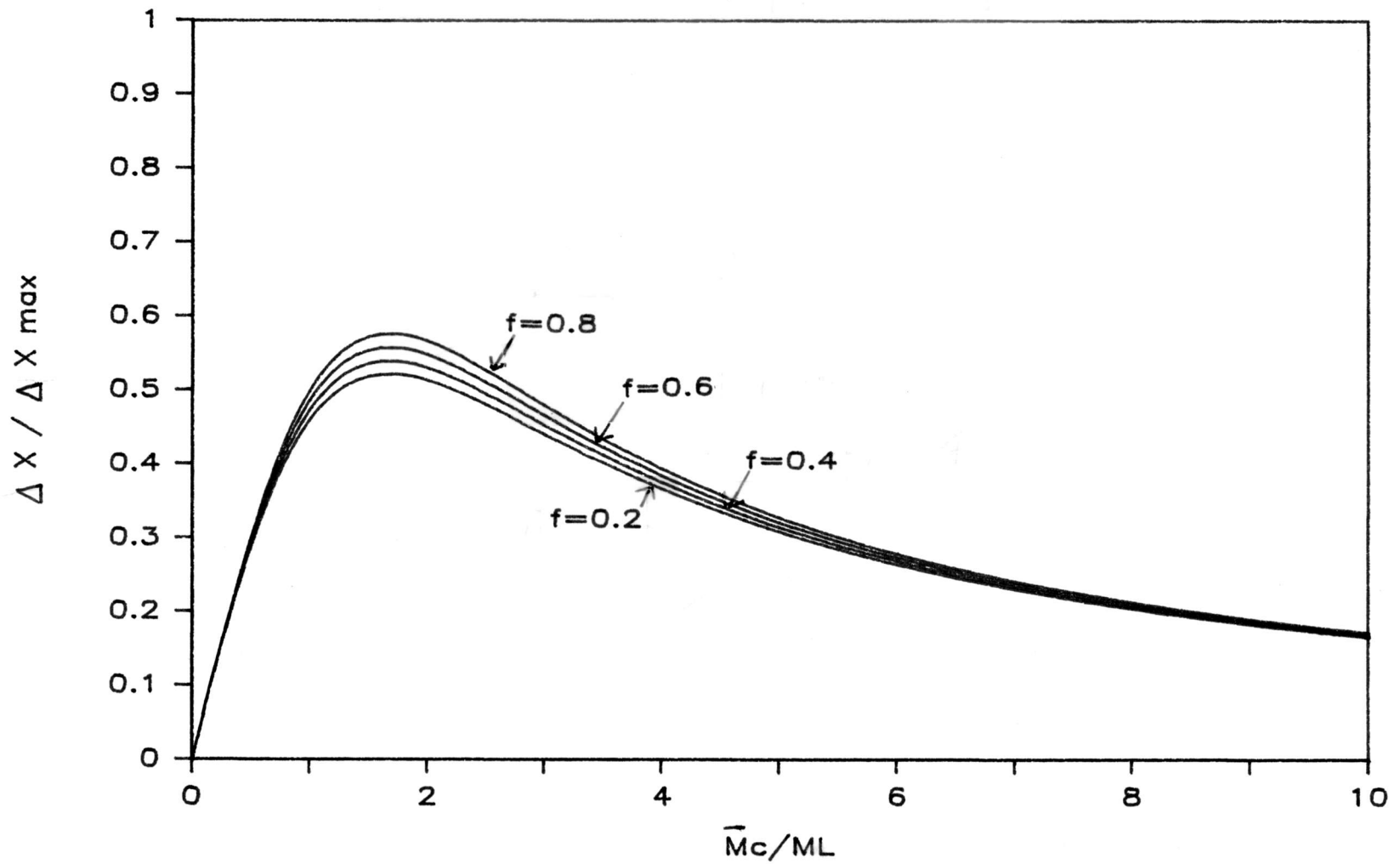
Figure 4.1   ΔX/ΔXmax for the $\overline{\phi}$f-Chart method
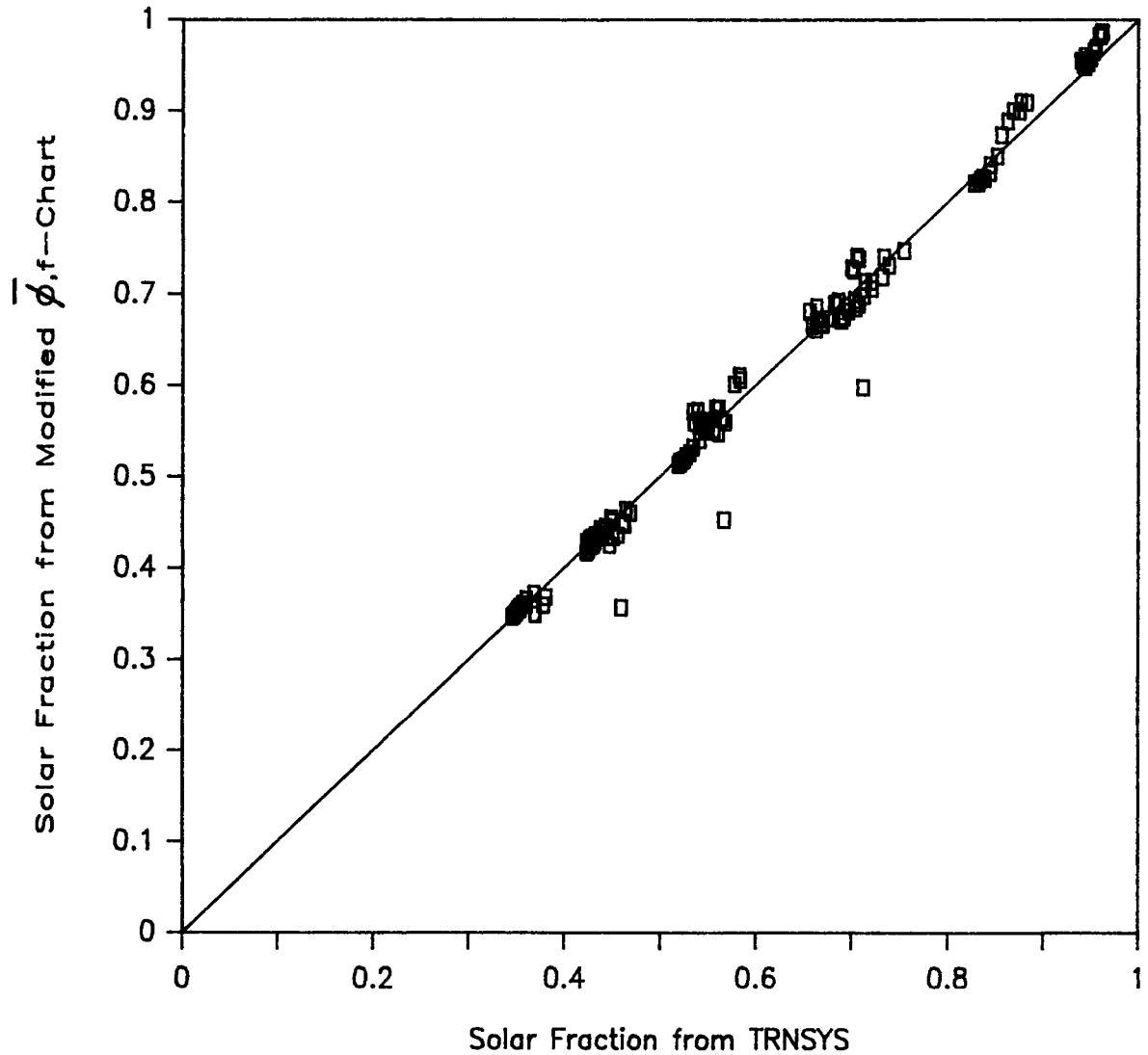
Figure 4.2   Annual Solar Fractions from TRNSYS Simulations
            Versus the $\bar{\phi}$f-Chart Method Modified with the
            Stratification Correction, for Mc=10-60 kg/hrm2
            and all Locations, Loads, and Systems.

stratified preheat tank appears to agree well with detailed simulations.

4.4 EXAMPLE

An example of estimating the performance of a stratified tank SDHW system using the $\overline{\phi}$,f-Chart method is presented here. The performance for a system having the parameter valued given in Table 4.2 will be estimated for the month of April. $\overline{R}$, R_n, and $r_{t,n}$ are determined as outlined in Reference [12]. For this example

$\overline{R}$=1.01

$r_{t,n}$=0.131

R_n=1.02

The monthly total load is

$L=M_d C_p (T_w - T_m) N$

=1.886 GJ

First, the mixed-tank solar fraction is obtained. Modifying F_R for the use conditions

F_R(use)/F_R(test)=0.841

$F_R U_L$= 3.98 W/m^{2}C

$F_R(\tau\alpha)$=0.677

An initial guess of 30°C is used for the monthly-average delivery temperature

Table 4.2. Parameter Values for System in $\bar{\phi}$, f-Chart Example

Location	Madison, Wisconsin
Meteorological	April
	$\bar{H}=14.90$ MJ/m^2
	$T_a=8.66°$ C
	$\bar{K}_t=0.47$
Collectors	$A_c=4.2$ m^2
	$F_R(\tau\alpha)_n=0.805$
	$\overline{(\tau\alpha)}/(\tau\alpha)/_n=.925$
	$(\tau\alpha)=.913$
	$F_R U_L=4.73$ W/m^{2}C
	$\dot{M}_c(\text{test})=71.5$ kg/hr m^2
	$\dot{M}_c(\text{use})=10$ kg/hr m^2
	slope=latitude=43.1°
Preheat Tank	Volume=0.30 m^3
	Height=1.5 m
	$U=0.42$ W/m^{2}C
	UA=2.75 W/C
Auxiliary Tank	negligible losses
Hot Water Load	Demand=300 ℓ/day
	$T_m=10$ C
	$T_w=60$ C
	$T_\infty=20$ C

$$f = \frac{Q_S}{L}$$

$$= \frac{(300)(4.19)(30-10)}{(300)(4.19)(60-10)}$$

$$=0.40$$

$$I_c = U_L(T_d-T_a)/(\overline{\tau\alpha})$$

$$=(3.98)(30-8.7)/((.677)(.925))$$

$$=135.5 \text{ W/m}^2$$

From this critical level, using Klein's correlation, equation 1.11, the maximum utilizability is

$$\overline{\phi}_{max}=0.691$$

The useful energy is calculated from equation 4.1

$$Q_{max} = \overline{\phi}_{max}A_cF_R(\overline{\tau\alpha})\overline{H}_tN$$

$$=29.7 \text{ MJ}$$

$$X = A_cF_RU_L(100°C)\Delta\tau/L$$

$$=2.30$$

$$a = 0.015 \frac{M_tC_P/A_c}{350.\text{kJ/m}^2°C}^{-0.76}$$

$$=0.0169$$

$$Z = L/(M_LC_p(100°C))$$

$$=0.50$$

$$Q_u = Q_{max}-a(e^{bf}-1.)(1.-e^{cX})(e^{dZ})L$$

$$=29.7-.0169[\exp(3.85\cdot0.4)-1]\cdot$$

$$[1-\exp(-.15 \cdot 2.30)]\exp(-1.959 \cdot 0.5)(1,886)/30$$

$$=29.29 \text{ MJ}$$

The tank lossed are estimated from equation 4.2 and 4.3

$$g = 0.2136 \left[\frac{M_t C_p / A_c}{350. \text{kJ}/\text{m}^2 {}^\circ\text{C}} \right]^{-0.704}$$

$$=0.239 \text{ C}$$

$$T_{tank} = T_d + g(e^{kf}-1.)(e^{hZ})$$

$$=30+(.239)[(\exp(4.702 \cdot 0.4)-]\exp(-4.002 \cdot 0.50)$$

$$=30.7 \text{ C}$$

$$Q_{LS} = (UA)_{tank}(T_{tank}-T_{env})$$

$$=(2.75)(30.2-20)(24)(3600)$$

$$=2.41 \text{ MJ}$$

A new guess of the delivery temperature can be obtained by averaging the initial supply temperature with the calculated supply temperature

$$Q_S = Q_U - Q_{LS}$$

$$=29.29-2.41$$

$$=26.88 \text{ MJ}$$

$$Q_S = \min[M_L C_p (T_d-T_{main}),L]$$

=25.14 MJ

$Q_{s,2}$ = (25.14 + 26.88)/2

=26.01 MJ

$T_{d,2} = T_{main} Q_s / M_L C_p$

=10 + 26,010/(300·4.19)

=30.69 C

Repeating the procedure with the new delivery temperature gives the following

f=.414

I_c=140.1 W/m^2

$\bar{\phi}_{max}$=.677

Q_{max}=29.1 MJ

Q_u=28.64 MJ

Q_{LS}=2.42 MJ

$T_{d,2}$=30.78 C

Since there was little change in the iterations, it is not

necessary to iterate further.

The next step is to calculate the monthly-average daily

collector to load flow ratio from equation 1.15 or 1.16 .

For this example, Klein's utilizability correlation was used

$$\frac{\bar{M}_c}{M_L} = \frac{\dot{M}_c}{M_L} -\bar{\phi}[A + B(R_n/\bar{R})][1. + 2CX_c] \bar{R}/(r_{tn} R_n)$$

$$=[(10)(4.2)/300](-.875)[-0.514+(-.990)(1.02/1.01)]\cdot$$

$$[1+2(0.330)(0.086)](1.01)/[(0.131)(1.02)]$$

$$=[(42kg/hr)/(300kg/day)]10.67 \ hrs/day$$

$$=1.49$$

Then $\Delta X/\Delta X_{max}$ can be determined from equation 4.11

$$\frac{\Delta X}{\Delta X_{max}} = \frac{0.6078 \ M}{[0.6019 \ M + -0.6019 \ f]^2 + 1.}$$

$$=0.549$$

The stratified tank heat removal factor and tank loss

coefficient are calculated from equations 4.9 and 4.11

$$(F_R U_L)_{str} = (F_R U_L)_{mix}(1.- \frac{\Delta X}{\Delta X_{max}})$$

$$=(3.98)(1-.549)$$

$$=1.80$$

$$(F_R)_{str} = \frac{\Delta X}{\Delta X_{max}} + (1.- \frac{Y_{str}-Y_{mix}}{Y_{max}-Y_{mix}}) \ (F_R)_{mix}.$$

$$[F_R(\tau\alpha)]_{str} = (0.549)(.913)+(1-0.549)(0.677)$$
$$=0.807$$

Going back to the $\overline{\phi}$,f-Chart method

f=0.40

I_c=51.4 W/m^2

$\overline{\phi}_{max}$=0.87

Q_{max}=44.8 MJ

Q_u=43.9 MJ

Q_{LS}=5.0 MJ

$T_{d,2}$=36.7 C

After a few iterations,

T_{min}=40.9 C

f=0.619

An increase of 20% from the mixed-tank solar fraction. The solar fraction from a TRNSYS simulation is 0.614.

CHAPTER FIVE: SUMMARY AND RECOMMENDATIONS

5.1 SUMMARY

The objective of this research was to develop a design method that could be used for solar domestic hot water heating systems that have thermally stratified preheat tanks. A high degree of stratification can be present for systems that have low collector flowrates, on the order of one fifth that of conventional SDHW systems. Low flow designs can achieve a performance 20% greater than an otherwise identical high collector flowrate system. Present design methods were developed assuming that the preheat tank is fully mixed, a good assumption with high collector flowrates. The mixed tank assumption will cause the design methods to underpredict the solar fraction from a stratified tank system.

A number of analytically derived equations have been developed to try to predict the performance of stratified tank systems. These equations cannot be used in design methods since the assumptions necessary in solving the differential equations give them limited applicability. The solar fraction differnce between a mixed-tank and a stratified tank system is a difficult variable to modify to

account for the increased performance of a stratified tank SDHW system. This is caused by its nonlinear behavior and dependence upon a number of variables.

A modification to the f-Chart method [4] that corrected for stratified tanks was presented in Chapter 3. A primary reason that stratified storage designs perform better than mixed tank systems is due to the reduced temperature of the fluid entering the collector. A lower collector inlet temperature reduces the thermal losses of the collector. A correction that modifed the collector loss coefficient and correspondingly, the heat removal factor was developed. This correction is a function of the monthly-average daily collector to load flow ratio and the solar fraction. The RMS error of the f-Chart method corrected with the collector loss coefficient modification compared to detailed simulations is 3.15% annually.

The $\bar{\phi}$,f-Chart design method was modified so that it can be used for stratified tank systems. A correction factor similar to that used for the f-Chart method was employed. The solar fraction error between the modified $\bar{\phi}$,f-Chart method and simulations is 2.1%.

5.2 RECOMMENDATIONS

Based on the results of this study several suggestions of areas for future research can be made. The plug-flow tank model ignores conduction through the tank walls, inlet mixing, and conduction through the fluid. For some systems, such as those with horizontal tanks, these effects may not be negligible. Systems with collector flowrates between that of a conventional system and that of a low-flow system may have some inlet mixing. A correction should be put in the plug-flow tank model to account for inlet mixing. More work should be done comparing experimental results with the performance of the plug-flow model to assertain the accuracy of the model over a wide range of system configurations.

This study examined two-tank SDHW systems. Other designs should be simulated and compared to the stratified tank design method. Indirect systems may perform better at high collector flowrates due to the increased heat exchanger efficiency and since in tank heat exchangers tend to reduce thermal stratification [2]. Single tank set-ups can be treated as two tanks in the mixed storage f-Chart method [6], but this should be investigated further for stratified tank systems. If the single tank has an in-tank heating element, the location of the element will influence the

degree of stratification. Other collector types should also be simulated and compared to the stratified tank design method.

REFERENCES

1   Cole, R.L. and Bellinger, J.O., "National Thermal Stratification in Tanks," Argonne National Lab, 82-7 (February 1982).

2   Fanney, A.H. and Klein, S.A., "Performance of Solar Domestic Hot Water Systems at the National Bureau of Standards Measurements and Predictions" ASME Journal of Solar Energy Engineering, 105, p. 311 (August 1983).

3   TRNSYS 12.1, Engineering Experiment Station Report 38-12, Solar Energy Laboratory, University of Wisconsin-Madison (1983).

4   Klein, S.A., Beckman, W.A. and Duffie, J.A., "A Design Procedure For Solar Heating Systems," Solar Energy, 18, 113 (1976).

5   Klein, S.A., and Beckman W.A., "A General Design Method for Closed-Loop Solar Energy Systems," Solar Energy, 22, 269 (1979).

6   Buckles, W.E., and Klein, S.A., "Analysis of Solar Domestic Hot Water Heaters", Solar Energy, 25 (May 1980).

7   Hottel, H.C., and Woertz, B.B., "Performance of Flat-plate Solar Heat Collectors," Trans. ASME, 64, 91 (1942).

8   Hottel, H.C., and Whillier, A., "Evalution of Flat-Plate Collector Performance," Transactions of Conference on Use of Solar Energy, Part 1, p. 74, University of Arizona Press (1958).

9   Bliss, R.W., "The Deriviation of Several Plate Efficiency Factors Useful in the Design of Flat-Plate Solar Heat Collectors." Solar Energy, 3, 55 (1959).

10 Liu, B.Y.H., and Jordan, R.C., "The Interrelationship and Characteristic Distribution of Direct, Diffuse, and Total Solar Radiation", Solar Energy, 6 (1960).

11   Klein, S.A. "Calculation of Flat-Plate Collector Utilizability," Solar Energy, 21, 393 (1978).

12   Duffie, J.A., and Beckman W.A., **"Solar Engineering of Thermal Processes"**, Wiley-Interscience, New York (1980).

13   Evans, D.L., Rule, T.T., and Wood, B.D., "A New Look at Long Term Collector Performance and Utilizability," Solar Energy, 28, 13 (1982).

14   Mitchell, J.C., Theilacker, J.C. and Klein, S.A., "Calculation of Monthly Average Collector Operating Time and Parasitic Energy Requirements," Solar Energy, 26, 555 (1981).

15   **F-Chart 4.1**, Engineering Experiment Station Report 50, Solar Energy Laboratory, University of Wisconsin-Madison (1980).

16   Erbs, D.G., Klein, S.A., and Beckman W.A., "Estimation of Degree-Days and Ambient Temperature Bin Data From Monthly-Average Temperatures" ASHRAE Journal, June (1983).

17   Phillips, W.F., "Effects of Stratification on the Performance of Solar Air Heating Systems." Solar Energy, 26, 175 (1981).

18   Hoerger, C.R., Phillips, W.F., "An Analytical Model for the Integrated Daily Performance of Solar Air Heating Systems." ASME Solar Conference (1984).

19   Phillips, W.F., and Dave R.N., "Effects of Stratification on the Performance of Liquid-Based Solar Heating Systems" Solar Energy, 29, No 2, pp. 111-120, (1982).

20   Veltkamp, W.B., "Thermal Stratification in Heat Storage," In C. den Ouden, **Thermal Storage of Solar Energy** , Martinus Nijhoff, The Hague, 2, 47 (1980).

21   Von Koppen, C.W.F., et al., "The Actual Benefits of Thermally Stratified Storage in A Small and A Medium Size Solar System," Proceedings ISES, Atlanta (1979).

22   Wuestling, M.D., Duffie, J.A., Klein, S.A. and Braun, J.E., "Investigation of Promising Control Alternatives for Solar Water Heating Systems," Proceedings of the ASES 1983 Annual Meeting, Minneapolis, Minnesota, Vol. 6, p. 229.

23   Turner, J.S., **Buoyancy Effects in Fluids**, Internal Mixing Processes, Cambridge University Press, pp. 313-337 (1973).

24   Lavan, Z., and Tompson, J., "Experimental Study of Thermally Stratified Hot Water Storage Tanks." Solar Energy, **19**, 519 (1977).

25   Fanney, A.H., written communication to S.A. Klein dated January 31, 1984

26   Morrison, G.L. and Braun, J.E., "System Modelling and Operation Characteristics of Thermosyphon Solar Water Heaters," submitted to Solar Energy (1984).

27   Mutch, J.J., "Residential Water Heating, Fuel Consumption Economics and Public Policy, RAND, Department R1498, NSF (1974).

28   Fischer, R.A., and Fanney, A.H., "Thermal Performance Comparisons for a Solar Hot Water System subjected to Various Hot Water Load Profiles", to be published in ASME Journal of Solar Energy Engineering.

29   Wuestling, M.D., "Investigation of Promising Control Alternatives For Solar Water Heating Systems," M.S. Thesis University of Wisconsin-Madison (1983).

30   Hall, I.J., et al., "Generation of a Typical Meteorological Year," Sandia National Laboratory, **Report SAND 78-1601** (1979).

31   Solar Rating and Certification Corporation, Directory of S.R.C.C. Certified Solar Collector Ratings, Washington D.C., **Fall 1983 Edition**.

32   Braun, J.E., Fanney, A.H., "Design and Evaluation of Thermosiphon Solar Hot Water Heating Systems", Proceedings of the ASES 1983 Annual Meeting, Minneapolis, Minnesota, Vol. 6, pp. 283-288.

33   "Energy Conservation in New Bulding Dessign," ASHRAE
      Standard 90A-1980, New York (1980).

34   Braun, J.E., Klein, S.A., and Pearson K.A., "An
      Improved Design Method for   Solar Water Heating
      Systems", Solar Energy, 31, 597 (1983).